

Florida State University Libraries

2024

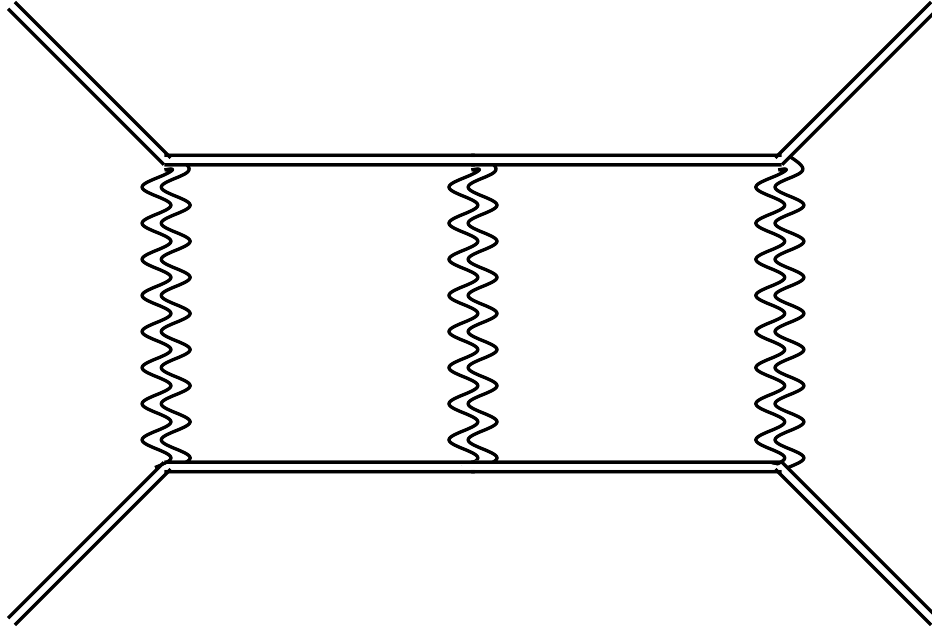
Parametrizations for Two-Loop Double-Box Feynman Integrals with Massive Particles

Robert Charles Laughlin



THE FLORIDA STATE UNIVERSITY
COLLEGE OF ARTS AND SCIENCES

**PARAMETRIZATIONS FOR TWO-LOOP DOUBLE-BOX
FEYNMAN INTEGRALS WITH MASSIVE PARTICLES**



By

ROBERT C. LAUGHLIN

A Thesis submitted to the
Department of Physics
in partial fulfillment of the requirements for graduation with
Honors in the Major.

Degree Awarded:
Spring, 2024

The members of the Defense Committee approve the thesis of Robert C. Laughlin,
defended on April 24, 2024.

Fernando Febres Cordero

Thesis Director

Olmo S. Zavala Romero

Outside Committee Member

Rachel Yohay

Committee Member

Takemichi Okui

Committee Member

Signatures are on file with the Honors Program office.

Contents

1	Introduction	4
2	Basics of Quantum Field Theory	5
2.1	Relativistic Approach to Quantum Mechanics	5
2.1.1	The Klein-Gordon Equation	6
2.1.2	The Dirac Equation	7
2.2	Lagrangian Density in Quantum Field Theory	8
2.2.1	Scalar Field Theory Lagrangian	8
2.2.2	Dirac Lagrangian	8
2.2.3	Electromagnetic Field Lagrangian	8
2.2.4	QED Lagrangian	9
2.3	The Hamiltonian	9
2.3.1	Scalar Field Hamiltonian	10
2.3.2	Dirac Hamiltonian	10
2.3.3	EM Hamiltonian	11
2.4	Theories with Interactions	12
2.4.1	Interaction Picture	12
2.4.2	Dyson Series	13
2.4.3	Interaction Example: $e^+ e^-$ production	13
2.5	Feynman Diagrams and Feynman Rules	14
2.5.1	Feynman Diagrams	14
2.5.2	QED Feynman Rules for Scattering Amplitudes	15
3	Feynman Integrals	16
3.1	Dimensional Regularization	16
3.1.1	Properties of Feynman Integrals in Dimensional Regularization	17
3.2	Feynman Integral Representations	18
3.2.1	Momentum Representation	18
3.2.2	Schwinger Representation	18
3.2.3	Feynman Representation	19
3.2.4	Lee-Pomeransky Representation:	20
3.2.5	Baikov Representation:	20
3.3	Integration By Parts Relations	22
3.3.1	IBP Example: One-Loop bubble	23
4	Einstein Hilbert Gravity	24
4.1	Feynman Rules for Einstein-Hilbert Gravity	24
4.2	Tree Level Graviton Scattering	25
5	Numerical Unitary Method and Integrand Parameterization	25
5.1	Cut-Equation	26
5.2	Adaptive Loop-Momentum Parametrizations	27
5.3	Tensor Basis	29
5.4	Scattering-Plane Tensor Basis	29
5.5	Master-Surface Basis	31
6	Numerical Unitary Method Applied to Double-Box	31
6.1	Double-Box Tensor Basis	32
6.2	Double-Box Scattering-Plane Tensor Basis	33
6.3	IBP Identities for Double-Box	34
6.4	Double-Box Master-Surface Basis	34
6.5	Cut Equation for Double-Box	35
6.5.1	ssSS Scattering Process	35

6.5.2	ssVV Scattering Process	36
6.6	Validation	36
6.7	Ancillary files	36
7	Conclusion and Outlook	37
	Appendices	38
A	Relativity	38
B	Alternate approach to Master-Surface Parametrization	40
C	Double-Box Tensor Basis	41
D	Double-Box Scattering Tensor Basis	42
E	IBP Identities for Double-Box	43
F	Double-Box Master-Surface Basis	45

Abstract

Using integration by parts identities, we construct a parametrization of amplitude integrands for a two-loop propagator structure. This parametrization directly reduces all related Feynman integrals to master integrals. This is a so-called master-surface integrand parametrization, where functions integrate either to master integrals or to zero. Our work has direct applications to the study of the conservative gravitational potential in a black hole binary system, in particular to its calculation at third order in Newton's constant $\mathcal{O}(G^3)$ employing scattering amplitude techniques and the generalized unitarity method.

1 Introduction

The merger of black holes in a binary system is one of the most extreme events in the cosmos. The merger is separated into three phases: *inspiral*, *merger*, and *ringdown*. During inspiral, the two black holes in the bounded orbit spiral inwards and converge on one another. During merger, the event horizons of the two black holes make contact and coalesce into a single body. During ringdown, the merged black hole relaxes into a stable state. Each stage of this process produce ripples in spacetime, similar to a tossed stone causing ripples in a pond. These ripples in spacetime are known as gravitational waves. Gravitational wave observatories (like the LIGO experiment) are designed to detect these gravitational waves. Figure 1 depicts the process together with the *waveform* that they produce and that can be detected far away by gravitational wave observatories.

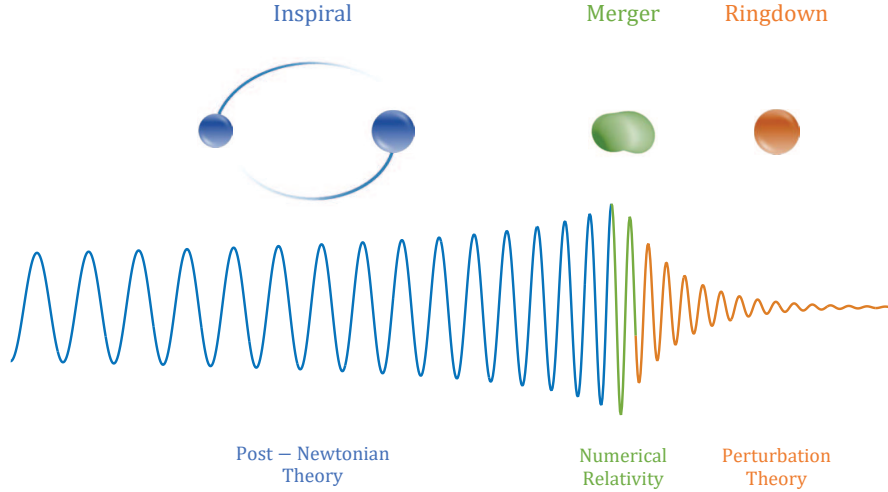
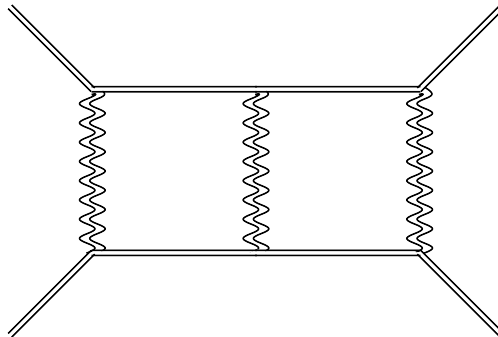


Figure 1: Three stages of the black hole merger: (i) Inspiral, (ii) Merger, (iii) Ringdown [5].

Recent observations of gravitational waves by LIGO have made precise theoretical calculations of the gravitational conservative potential for a compact binary system increasingly valuable. Similar to an elementary particle, black holes are described with a mass, spin, and charge. During the inspiral stage of the merger, when the distance between the black holes is large with respect to the size of the event horizons of the black holes, it becomes possible to treat these black holes like point-like particles. In addition, there is common information in the conservative gravitational potential of a bound and of an open binary system (for example between two black holes), meaning we can use the potential calculated by scattering black holes to learn about the potential between bound binary black hole systems. This suggests that we can exploit the tools of Quantum Field Theory (QFT) to compute scattering amplitudes to help us solve for the potential between binary bound black hole systems, providing us with very precise forms for the gravitational potential $V(r)$.



The Feynman diagram before defines the *double-box* diagram that we study. In the figure, the solid double lines represent the point-like massive particles that we use to represent the black holes in the scattering process, while the wiggling lines represent graviton (the gravitational force carrier) exchanges.

In the rest of this document we will focus on an specific analysis related to the precision program for gravitational wave astronomy. In calculations done using scattering amplitudes, fundamental building blocks are the so called Feynman integrals. We will introduce how these integrals appear in the context of perturbative quantum field theory, using scalar field theory and quantum electrodynamics as working examples. Afterwards we make an in-depth analysis of the calculus of Feynman integrals, presenting the tools required to build a powerful parametrization for the key double-box family of Feynman integrals that are required for the calculation of the conservative potential for a compact binary system at $\mathcal{O}(G^3)$, where G is Newton's constant. The double-box family includes propagators for two types of massive particles (representing the black holes being scattered) and massless particles (representing graviton exchanges), built from an effective field theory based on the Einstein-Hilbert (EH) Lagrangian.

2 Basics of Quantum Field Theory

In studying elementary particles, before we can fuss about the interactions between particles, we first get a grasp on how particles behave in the absence of all interactions. In classical mechanics, we do this by finding the Lagrangian of this particle. In QFT, we do the same thing, first targeting a *free* version for the Lagrangian density. To build the Lagrangian for relativistic theories of quantum mechanics, we build on some of the concepts we learned in our undergraduate quantum mechanics and explore their shortcomings in relativistic extensions. Then we will develop new theoretical frameworks until we arrive at a Lagrangian for free field theories from which we will develop our understanding of QFT.

2.1 Relativistic Approach to Quantum Mechanics

When you are introduced to elementary particles in undergraduate physics, you are typically taught about them in the context of Schrödinger's equation:

$$i\hbar \frac{\partial}{\partial t} \Psi(\vec{x}, t) = \left(-\frac{\hbar^2}{2m} \nabla^2 + V \right) \Psi(\vec{x}, t) .$$

In high-energy physics, we typically use what are called natural units. Natural units set $\hbar = c = 1$, and we will use such units throughout the rest of the paper unless otherwise specified. We also typically analyze particles that are “free”, i.e. in the absence of a potential, so that $V = 0$. Schrödinger's equation for a free particle using natural units is expressed as:

$$i \frac{\partial}{\partial t} \Psi(\vec{x}, t) = -\frac{1}{2m} \nabla^2 \Psi(\vec{x}, t) . \quad (2.1)$$

Such an equation has plane-wave solutions of the form

$$\Psi \propto e^{i(\vec{p} \cdot \vec{x} - Et)} , \quad (2.2)$$

where $E = \frac{p^2}{2m}$. These types of solutions will play a critical role later on.

Schrödinger's equation works well for analyzing low-energy systems; however, in the high-energy regime, we must introduce special relativity into the picture. When thinking in terms of relativity, Schrödinger's equation is insufficient for several reasons.

First, we note that in special relativity time and space are treated under equal footing, and put together into 4-vectors $x^\mu = (t, \vec{x})$ representing *spacetime*. Therefore, we should expect that any fundamental differential equation would have the same order in both space in time. However, we can see in equation (2.1) that Schrödinger's equation is first-order in time derivatives and second-order in space derivatives. This means that Schrödinger's equation is not relativistically covariant.

Furthermore, there is a problem relating to the probability of finding a particle in quantum mechanics. The probability density of a particle is given by,

$$\rho(\vec{x}, t) = |\Psi(\vec{x}, t)|^2 . \quad (2.3)$$

We can integrate equation (2.3) over all of space to find the probability of finding a particle anywhere in space,

$$\int |\Psi(\vec{x}, t)|^2 dV . \quad (2.4)$$

When integrating over all of space, this equation is normalized to one, as we expect the particle must be somewhere. Generically, however, equation (2.4) depends on time. This suggests that either the probability of finding the particle should change with time, or the normalization should change over time. However, Schrödinger's equation actually ensures conservation of this total probability. Consider the 4-vector current defined as

$$j^\mu = (\rho, \vec{j}) = \left(|\Psi|^2, -\frac{i}{2m} (\Psi^* \nabla \Psi - \Psi \nabla \Psi^*) \right) . \quad (2.5)$$

Schrödinger's equation implies that this current is conserved, that is $\partial_\mu j^\mu = 0$. So even if we integrate over space $\int \partial_\mu j^\mu dV = 0$. From this, we conclude that

$$\frac{d}{dt} \left(\int |\Psi|^2 dV \right) = 0 , \quad (2.6)$$

because the extra term should be a surface term that should vanish. This means that $\int |\Psi|^2 dV$ is constant and normalizable to unity. While conservation of the total probability might be seen as a good feature, it leads to the downfall of this version of quantum mechanics in the relativistic regime.

As observed through the photoelectric effect, in real life particles appear and disappear. If we were to have sufficient energy in a photon to create an electron-positron pair, then the initial and final probability of finding an electron would be given by

$$\left(\int |\Psi|^2 dV \right)_{initial} = 0 , \quad (2.7)$$

and

$$\left(\int |\Psi|^2 dV \right)_{final} = 1 . \quad (2.8)$$

However, this violates the conservation of probability current we previously established. Therefore, quantum mechanics breaks down in the relativistic regime, where there is enough energy to create new particles. This necessitated a new theory to replace non-relativistic quantum mechanics.

2.1.1 The Klein-Gordon Equation

We can use some of the information we know from special relativity and quantum mechanics to try to find a framework consistent with the two. First, we still favor the existence of plane wave solution, equation (2.2), that we saw from quantum mechanics, which we re-express in a covariant form, that is, consistent with special relativity,

$$\phi \propto e^{i(p_\mu x^\mu)} , \quad (2.9)$$

where we have introduced the momentum 4-vector, $p = (E, \vec{p})$. Second, using the relativistic dispersion relation, equation (A.11), we conclude that p^μ must fulfill

$$p_\mu p^\mu = m^2 . \quad (2.10)$$

These two expected results can be used to propose a new dynamical equation for the function ϕ ,

$$(\partial_\mu \partial^\mu + m^2) \phi(x) = 0 . \quad (2.11)$$

This equation is called the Klein-Gordon Equation. This equation presents another problem which is perhaps bigger than the problems we faced from Schrödinger's equation. This equation, for a given 3-momentum \vec{p} , has two plane-wave solutions of the form

$$\phi \propto e^{i(\pm Et - \vec{p} \cdot \vec{x})} , \quad (2.12)$$

where $E = \sqrt{\vec{p} \cdot \vec{p} + m^2}$. These can be seen as positive- and negative-energy solutions of the relativistic dispersion relationship. However, if there are particles with unbound negative energy nothing is stopping any physical system from decaying into these negative-energy particles. This means that the physical system would be unstable [13]!

2.1.2 The Dirac Equation

Paul Dirac proposed a dynamics equation that instead of being second-order in the time and space derivatives (as the Klein-Gordon equation), it would be first-order in time and space derivatives. It would be such that in its square, you would recover Klein-Gordon's equation. This gave the differential equation for the function ψ

$$(i\gamma^\mu \partial_\mu - m)\psi = 0 . \quad (2.13)$$

This equation is known as the Dirac Equation. Here ψ is known as the Dirac spinor and is a 4-component object. γ^μ is known as the Gamma matrices which fulfill the property

$$\{\gamma^\mu, \gamma^\nu\} = 2\eta^{\mu\nu} , \quad (2.14)$$

where $\eta^{\mu\nu}$ is the metric tensor defined in equation (A.5) in the Appendix. In a particular representation of the gamma matrices, called the Dirac representation, the gamma matrices take the form

$$\gamma^0 = \begin{bmatrix} \mathbb{1} & 0 \\ 0 & -\mathbb{1} \end{bmatrix} , \quad (2.15)$$

$$\gamma^i = \begin{bmatrix} 0 & \sigma_i \\ -\sigma_i & 0 \end{bmatrix} , \quad (2.16)$$

where $\mathbb{1}$ is the 2×2 identity matrix and σ_i ($i = 1, 2, 3$) are the Pauli matrices from quantum mechanics. If we look for plane wave solutions to the Dirac equation

$$\phi = u(p) e^{i p_\mu x^\mu} , \quad (2.17)$$

plugging into equation (2.13), we get

$$(-\gamma^\mu p_\mu - m) u(p) = 0 .$$

In the reference frame where $\vec{p} = 0$, using $E = \pm m$, we can reduce this to

$$(-\gamma^0 E - m) u = (\mp \gamma^0 m - m) u = 0 .$$

For $E = +m$ we get solutions u of the form

$$u = \begin{bmatrix} A_1 \\ A_2 \\ 0 \\ 0 \end{bmatrix} , \quad (2.18)$$

and for $E = -m$ we get solutions u of the form

$$u = \begin{bmatrix} 0 \\ 0 \\ A_1 \\ A_2 \end{bmatrix} . \quad (2.19)$$

Dirac interpreted these solutions as spin-up (A_1) and spin-down (A_2) particles (fermions), for the $E = +m$ solutions. On the other hand, he introduced the idea of anti-particles (anti-fermions) as related to the $E = -m$ solutions. To explain how these negative-energy solutions would not produce an unstable theory, Dirac argued that using Pauli's exclusion principle and assuming the existence of what is known as *the Dirac sea*, where these negative energy states are by default filled, then there

could be no transition to them as Pauli's principle would exclude it. When a photon with sufficient energy interacts with the Dirac sea, this negative energy particle is raised to a total positive energy state producing a fermion and leaving a "hole" in the Dirac sea. This hole is a new type of particle, the anti-particle (anti-fermion). To maintain local conservation of charge, these anti-fermions must have opposite charges as their fermion counterparts [13]. This interpretation can help us describe some physical systems, but they are always a type of effective description.

2.2 Lagrangian Density in Quantum Field Theory

To overcome the difficulties described before, related to negative-energy solutions to the equations of motion of the functions ϕ (for the Klein-Gordon equation) and ψ (for the Dirac equation), we introduce the concept of the *quantum field*. That is, the objects $\phi(x)$ and $\psi(x)$ are promoted to operators labelled by the spacetime argument x . And for them, we build Lagrangian densities, which classically (still thinking of $\phi(x)$ and $\psi(x)$ as functions) give their corresponding equation of motion.

2.2.1 Scalar Field Theory Lagrangian

We construct a Lagrangian density for a classical scalar field ϕ of the form:

$$\mathcal{L} = \frac{1}{2} \partial_\mu \phi \partial^\mu \phi - \frac{1}{2} m^2 \phi^2 . \quad (2.20)$$

This Lagrangian density implies an equation of motion for the field ϕ which is the Klein-Gordon equation outlined before. To see this we make use of the Euler-Lagrange equation of motion

$$\frac{\partial \mathcal{L}}{\partial \phi} - \partial_\mu \frac{\partial \mathcal{L}}{\partial (\partial_\mu \phi)} = 0 , \quad (2.21)$$

plugging in equation (2.20) into equation (2.21) we get

$$\begin{aligned} \frac{\partial \mathcal{L}}{\partial \phi} &= -m^2 \phi , \\ \frac{\partial \mathcal{L}}{\partial (\partial_\mu \phi)} &= \frac{1}{2} (\partial^\mu \phi + \partial^\mu \phi) = \partial^\mu \phi , \\ \Rightarrow -m^2 \phi - \partial_\mu (\partial^\mu \phi) &= 0 , \\ \Rightarrow (\partial_\mu \partial^\mu + m^2) \phi &= 0 . \end{aligned} \quad (2.22)$$

which is just the Klein-Gordon equation, equation (2.11) we introduced before.

2.2.2 Dirac Lagrangian

We can also construct a Lagrangian density which implies an equation of motion matching Dirac's equation introduced before. It has the following structure:

$$\mathcal{L}_{Dirac} = \bar{\psi} (i \not{\partial} - m) \psi \quad (2.23)$$

where $\bar{\psi} = \psi^\dagger \gamma^0$ and $\not{\partial} = \gamma^\mu \partial_\mu$. This Lagrangian density is a starting point to build one for the theory of quantum electrodynamics (QED) as we discuss next.

2.2.3 Electromagnetic Field Lagrangian

In QED we wish to study how electrons interact with electromagnetic fields. The Lagrangian associated with the electromagnetic field is given by

$$\mathcal{L}_{EM} = -\frac{1}{4} F^{\mu\nu} F_{\mu\nu} , \quad (2.24)$$

where $F^{\mu\nu}$ is the electromagnetic field strength tensor, which is defined by

$$F_{\mu\nu} \equiv \partial_\mu A_\nu - \partial_\nu A_\mu . \quad (2.25)$$

Here A^μ is electromagnetic four-potential, which combines the scalar and vector potentials for electricity and magnetism into a single four-vector, $A^\mu = (\varphi, \mathbf{A})$. From this definition we see that $F_{\mu\nu}$ is a rank-2 Lorentz tensor with components

$$F_{\mu\nu} = \begin{bmatrix} 0 & -E_x & -E_y & -E_z \\ E_x & 0 & -B_z & B_y \\ E_y & B_z & 0 & -B_x \\ E_z & -B_y & B_x & 0 \end{bmatrix} . \quad (2.26)$$

From the Electromagnetic Field Lagrangian, we are able to recover Maxwell's equation. Using $F_{\mu\nu}$, Maxwell's equations in the covariant form are given by

$$\begin{aligned} \partial_\nu F^{\mu\nu} &= j^\mu , \\ \epsilon^{\sigma\mu\nu\rho} \partial_\mu F_{\nu\rho} &= 0 . \end{aligned} \quad (2.27)$$

where $j^\mu = (\rho, \mathbf{J})$ and $\epsilon^{\sigma\mu\nu\rho}$ is the 4-dimensional Levi-Civita symbol. Using our relations between \mathbf{E} and \mathbf{B} and their scalar and vector potentials,

$$\mathbf{E} = -\vec{\nabla}\varphi + \dot{\mathbf{A}} , \quad (2.28)$$

$$\mathbf{B} = \nabla \times \mathbf{A} , \quad (2.29)$$

we see that equation (2.27), is the same as the Maxwell equations we learned in undergraduate Electricity and Magnetism,

$$\begin{aligned} \nabla \cdot \mathbf{E} &= \rho , \\ \nabla \cdot \mathbf{B} &= 0 , \\ \nabla \times \mathbf{E} &= -\dot{\mathbf{B}} , \\ \nabla \times \mathbf{B} &= \mathbf{J} + \dot{\mathbf{E}} . \end{aligned} \quad (2.30)$$

We will use the Lagrangian \mathcal{L}_{EM} in constructing the Lagrangian of QED.

2.2.4 QED Lagrangian

To illustrate the building of a quantum field theory, we will use a Lagrangian for the theory of quantum electrodynamics (QED). It employs the structure of the Dirac Lagrangian and the electromagnetic field Lagrangian introduced before. More precisely, it is given by

$$\mathcal{L}_{QED} = \bar{\psi} (i\rlap{\not{D}} - m) \psi - \frac{1}{4} F^{\mu\nu} F_{\mu\nu} , \quad (2.31)$$

where $\rlap{\not{D}} = \gamma^\mu D_\mu$ with $D_\mu = (\partial_\mu - ieA_\mu)$. The term $\bar{\psi}\rlap{\not{A}}\psi$ couples the electron (fermion) from the Dirac equation to the photon from Maxwell's equations and allows us to understand the interaction between fermions and the photon, the carrier of the electromagnetic force. We are able to do this because \mathcal{L}_{QED} is invariant under gauge transformations where both ψ and A^μ transform accordingly. This Lagrangian will be used to build up an example of QFT.

2.3 The Hamiltonian

While we move forward in the construction of a quantum theory consistent with relativity, we start studying the structure of the Hamiltonians for the theories with the Lagrangians that we have introduced before. Our Hamiltonian we express in terms of a Hamiltonian density, \mathcal{H} , according to

$$H = \int d^3x \mathcal{H} , \quad (2.32)$$

where the Hamiltonian density, \mathcal{H} , is defined by

$$\mathcal{H}(\phi, \Pi) = \Pi \dot{\phi} - \mathcal{L} , \quad (2.33)$$

where $\Pi = \partial \mathcal{L} / \partial \dot{\phi}$ is the conjugated momentum field associated with our Lagrangian and field ϕ . Until this point our fields (like ϕ and Π) are classical functions of spacetime.

2.3.1 Scalar Field Hamiltonian

For a scalar field Lagrangian, equation (2.20), we start by using the plane wave solution for ϕ , here a classical function,

$$\phi(x) = \int \frac{d^3 p}{(2\pi)^3 2\omega} \left(a(\vec{p}) e^{-ip_\mu x^\mu} + a(\vec{p})^* e^{ip_\mu x^\mu} \right) , \quad (2.34)$$

where $a(\vec{p})$ and $a(\vec{p})^*$ are the coefficients to our plane wave solution, and $\omega = \sqrt{|\vec{p}|^2 + m^2}$. We now want to promote ϕ to a field, which is an operator labeled by spacetime components. To do so, we make use of our canonical quantization commutation relations

$$\begin{aligned} [\phi(\vec{x}, t), \phi(\vec{y}, t)] &= 0, \\ [\Pi(\vec{x}, t), \Pi(\vec{y}, t)] &= 0, \\ [\phi(\vec{x}, t), \Pi(\vec{y}, t)] &= i\delta^3(\vec{x} - \vec{y}). \end{aligned} \quad (2.35)$$

Through this process we promote $a(\vec{p})$ and $a(\vec{p})^*$ to operators, $a_{\vec{p}}$ and $a_{\vec{p}}^\dagger$. Then, we can express the quantum field ϕ as

$$\phi_i = \int \frac{d^3 p}{(2\pi)^3 2\omega} \left(a_{\vec{p}} e^{-ip_\mu x^\mu} + a_{\vec{p}}^\dagger e^{ip_\mu x^\mu} \right) , \quad (2.36)$$

where $a_{\vec{p}}$ is the annihilation operator, $a_{\vec{p}}^\dagger$ is the creation operator. We derive commutator relations for our creation and annihilation operators using our canonical commutation relations, equation (2.35),

$$\begin{aligned} [a_{\vec{p}}, a_{\vec{p}'}] &= 0, \\ [a_{\vec{p}}^\dagger, a_{\vec{p}'}^\dagger] &= 0, \\ [a_{\vec{p}}, a_{\vec{p}'}^\dagger] &= (2\pi)^3 2\omega \delta^3(\vec{p} - \vec{p}') . \end{aligned} \quad (2.37)$$

The creation and annihilation operators either create one-particle states or annihilate the “ground state” of our system, the ket $|0\rangle$, which we call the “vacuum”:

$$\begin{aligned} a_{\vec{p}}|0\rangle &= 0, \\ a_{\vec{p}}^\dagger|0\rangle &= |\vec{p}\rangle. \end{aligned} \quad (2.38)$$

From these results, using equation (2.32) and (2.33) and simplifying, we can solve for the Hamiltonian to be

$$H = \int \frac{d^3 p}{(2\pi)^3 2\omega} \omega a_{\vec{p}}^\dagger a_{\vec{p}} , \quad (2.39)$$

Where H is *normal ordered*, typically denoted by $:H:$, where the creation operators are listed before the annihilation operators [13]. $a_{\vec{p}}^\dagger a_{\vec{p}}$ is known as the *number operator* as it tells us the number of particles with momentum p in our system.

2.3.2 Dirac Hamiltonian

For \mathcal{L}_{Dirac} our Dirac spinor is expressed as

$$\psi_i(x) = \sum_{s=\pm} \int \frac{d^3 p}{(2\pi)^3 2\omega} \left(c(\vec{p})^s u_i(\vec{p})^s e^{-ip_\mu x^\mu} + d(\vec{p})^{s*} v_i(\vec{p})^s e^{ip_\mu x^\mu} \right) , \quad (2.40)$$

where $u_i(\vec{p})^s$ and $v_i(\vec{p})^s$ are spinor coefficients and $c(\vec{p})^s$ and $d(\vec{p})^{s*}$ are coefficients to our plane wave solution. Using the same process as with a scalar particle of promoting the classical function ψ to a quantum field by imposing the canonical commutation relations,

$$\psi_i = \sum_{s=\pm} \int \frac{d^3p}{(2\pi)^3 2\omega} \left(c_{\vec{p}}^s u_{i,\vec{p}}^s e^{-ip_\mu x^\mu} + d_{\vec{p}}^{s\dagger} v_{i,\vec{p}}^s e^{ip_\mu x^\mu} \right), \quad (2.41)$$

where $u_{i,\vec{p}}^s$ and $v_{i,\vec{p}}^s$ are spinors and $c_{\vec{p}}^s$ and $d_{\vec{p}}^{s\dagger}$ are the annihilation and creation operators for two separate particles. We derive the Hamiltonian for the Dirac Lagrangian to be

$$H = \int \frac{d^3p}{(2\pi)^3 2\omega} \omega \left(c_{\vec{p}}^\dagger c_{\vec{p}} - d_{\vec{p}}^\dagger d_{\vec{p}} \right). \quad (2.42)$$

However, from our understanding that the Hamiltonian relates to energy from Quantum Mechanics, the $-$ in this expression once again suggests negative energy. This is clearly nonphysical, so Dirac made the “bold step” and concluded that for spinor fields, our commutator operator is replaced with the anti-commutator operator, which implies for the pair of creation/annihilation operators

$$\begin{aligned} \{c_{\vec{p}}^s, c_{\vec{p}'}^{s'\dagger}\} &= (2\pi)^3 2\omega \delta^3(\vec{p} - \vec{p}') \delta^{ss'}, \\ \{d_{\vec{p}}^s, d_{\vec{p}'}^{s'\dagger}\} &= (2\pi)^3 2\omega \delta^3(\vec{p} - \vec{p}') \delta^{ss'}, \end{aligned} \quad (2.43)$$

where any other combination of anti-commutators vanish. Under this prescription, we find the true Hamiltonian corresponding to the Dirac Lagrangian,

$$H = \int \frac{d^3p}{(2\pi)^3 2\omega} \omega \left(c_{\vec{p}}^\dagger c_{\vec{p}} + d_{\vec{p}}^\dagger d_{\vec{p}} \right). \quad (2.44)$$

From this, we understand that $c_{\vec{p}}^\dagger$ and $c_{\vec{p}}$ are the creation and annihilation operators associated with the fermion and $d_{\vec{p}}^\dagger$ and $d_{\vec{p}}$ are the creation and annihilation operators associated with the anti-fermion. In this description all single-particle (or single anti-particle) states (and therefore all multiparticle states) have positive energy.

2.3.3 EM Hamiltonian

When we compute the Hamiltonian density of our \mathcal{L}_{EM} we obtain,

$$\mathcal{H} = \frac{1}{2} \left(|\vec{E}|^2 + |\vec{B}|^2 - A_0 \vec{\nabla} \cdot \vec{E} \right). \quad (2.45)$$

As we can see the A_0 component of our field is non-dynamical, it has in particular no time derivatives. From this, we end up with a quantum field for the photons as

$$A_i = \sum_s \int \frac{d^3p}{(2\pi)^3 2\omega} \left(a_{\vec{p}}^s \epsilon_i^{s*} e^{-ip_\mu x^\mu} + a_{\vec{p}}^{s\dagger} \epsilon_i^s e^{ip_\mu x^\mu} \right), \quad (2.46)$$

where $a_{\vec{p}}^s$ and $a_{\vec{p}}^{s\dagger}$ are the annihilation and creation operators for the photon and ϵ_i^s is the polarization vectors for the photon.

In a very similar way to the scalar field, we arrive at the normal ordered Hamiltonian for the electromagnetic field to be

$$H = \int \frac{d^3p}{(2\pi)^3 2\omega} \omega a_{\vec{p}}^\dagger a_{\vec{p}}, \quad (2.47)$$

with $\omega = \sqrt{|\vec{p}|^2}$. We now wish to add operators to our Lagrangians which will allow interactions among fields.

2.4 Theories with Interactions

2.4.1 Interaction Picture

Using operator algebra in quantum mechanics, states can evolve in the following manner

$$|\phi(t)\rangle = U(t, t_0) |\phi(t_0)\rangle , \quad (2.48)$$

where $|\phi(t_0)\rangle$ is the initial state, $|\phi(t)\rangle$ is the final state, and $U(t, t_0)$ is so-called evolution operator which translates between them.

The probability of finding a particle initially in the state $|\phi(t_0)\rangle$ later on in the state $|\psi(t)\rangle$ is given by

$$\text{Prob} = |\langle\psi(t)|U(t, t_0)|\phi(t_0)\rangle|^2 . \quad (2.49)$$

The Schrödinger picture, where states evolve with time and operators do not, this $U(t, t_0)$ is related to the Hamiltonian by,

$$i \frac{d}{dt} U(t, t_0) = H U(t, t_0) . \quad (2.50)$$

which we solve by,

$$U(t, t_0) = e^{-iH(t-t_0)} . \quad (2.51)$$

In the Heisenberg picture, where operators evolve with time and states do not, we find that states in this picture are related to states in the Schrödinger picture by

$$|\phi\rangle_H = e^{iH(t-t_0)} |\phi\rangle_s . \quad (2.52)$$

Operators in the Heisenberg picture are related to operators in the Schrödinger picture by

$$\mathcal{O}_H = e^{iH(t-t_0)} \mathcal{O}_S e^{-iH(t-t_0)} , \quad (2.53)$$

where \mathcal{O}_H is some generic time-dependent operator in the Heisenberg picture corresponding to a time-independent operator \mathcal{O}_S in the Schrödinger picture.

There is another picture particularly helpful for studying theories with interactions (extra operators added to a given Hamiltonian). In the so-called interaction picture, we split the interaction term of our Hamiltonian, H_1 , from the free term of our Hamiltonian, H_0 , so that

$$H = H_0 + H_1 . \quad (2.54)$$

We then define how states in the interaction picture are related to states in the Schrödinger picture by

$$|\phi\rangle_I = e^{iH_0 t} |\phi\rangle_s , \quad (2.55)$$

where we have set $t_0 = 0$ without loss of generality. Now

$$\mathcal{O}_I = e^{iH_0 t} \mathcal{O}_S e^{-iH_0 t} . \quad (2.56)$$

The corresponding evolution operator $U_I(t, t_0)$ in this picture fulfills

$$\begin{aligned} i \frac{d}{dt} U_I(t, t_0) &= H_I U_I(t, t_0) \\ \frac{d}{dt} U_I(t, t_0) &= -i H_I U_I(t, t_0) \end{aligned} \quad (2.57)$$

where H_I is H_1 in the interaction picture. By integration, we then find

$$U_I(t, t_0) = \mathbb{1} - i \int_{t_0}^t dt H_I(t) U_I(t, t_0) . \quad (2.58)$$

2.4.2 Dyson Series

We to solve for U_I iteratively using equation (2.58), and get

$$\begin{aligned} U_I(t, t_0) = & \mathbb{1} - i \int_{t_0}^t dt_1 H_I(t_1) + (-i)^2 \int_{t_0}^t dt_1 \int_{t_0}^{t_1} dt_2 H_I(t_1) H_I(t_2) + \dots \\ & + (-i)^m \int_{t_0}^t dt_1 \dots \int_{t_0}^{t_{m-1}} dt_m H_I(t_1) \dots H_I(t_m) + \dots \end{aligned} \quad (2.59)$$

We then introduce a time ordering operator, T , such that

$$\int_{t_0}^t dt_1 \dots \int_{t_0}^{t_{m-1}} dt_m H_I(t_1) \dots H_I(t_m) = \frac{1}{m!} \int_{t_0}^t dt_1 \dots \int_{t_0}^{t_{m-1}} dt_m T\{H_I(t_1) H_I(t_2) \dots H_I(t_m)\} , \quad (2.60)$$

where $T\{H_I(t_1) H_I(t_2) \dots H_I(t_m)\}$ takes the form

$$T\{H_I(t_1) H_I(t_2) \dots H_I(t_m)\} = \begin{cases} H_I(t_1) H_I(t_2) \dots H_I(t_m) & \text{if } t_1 > t_2 > \dots > t_m \\ H_I(t_2) H_I(t_1) \dots H_I(t_m) & \text{if } t_2 > t_1 > \dots > t_m \\ \vdots & \end{cases} \quad (2.61)$$

With this we have the formal solution for U_I as a *Dyson series*:

$$U_I(t, t_0) = T \exp \left(-i \int_{t_0}^t dt' H_I(t') \right) . \quad (2.62)$$

We can now use this to analyze interactions and study the evolution of asymptotic states $|i\rangle$ and $|f\rangle$, where $|i\rangle$ is the initial state $t \rightarrow -\infty$ and $|f\rangle$ is the final state $t \rightarrow \infty$. The transition amplitude between $|i\rangle$ and $|f\rangle$, is given by

$$A = \langle f | U_I(+\infty, -\infty) | i \rangle . \quad (2.63)$$

2.4.3 Interaction Example: $e^+ e^-$ production

To get a better sense of interactions, we will analyze $e^+ e^-$ production from a photon.

$$\gamma(p_\gamma) \rightarrow e^+(p_+) e^-(p_-) , \quad (2.64)$$

so our initial and final states are given by

$$\begin{aligned} |i\rangle &= a_{p_\gamma}^\dagger |0\rangle , \\ |f\rangle &= c_{p_-}^\dagger d_{p_+}^\dagger |0\rangle . \end{aligned} \quad (2.65)$$

Starting from the QED Lagrangian we will try to get our interaction term. Starting with our QED Lagrangian, equation (2.31), and applying the definition of \not{D} ,

$$\begin{aligned} \mathcal{L}_{QED} &= \bar{\psi} (i\not{D} - m) \psi - \frac{1}{4} F^{\mu\nu} F_{\mu\nu} , \\ \mathcal{L}_{QED} &= \bar{\psi} (i\not{\partial} - m) \psi - \frac{1}{4} F^{\mu\nu} F_{\mu\nu} - ie\bar{\psi} \not{A} \psi , \end{aligned} \quad (2.66)$$

where, e is the charge of our fermion, here an electron. Our first term is our free fermion term, the second term is our free photon term, and our last term is our interaction term. To explore this interaction, we apply a perturbation theory. To the zeroth order for “ e ”:

$$\begin{aligned} \langle f | U | i \rangle_{\mathcal{O}(0)} &= \langle 0 | c_{p_-} d_{p_+} a_{p_\gamma}^\dagger | 0 \rangle \\ &= \langle 0 | c_{p_-} a_{p_\gamma}^\dagger d_{p_+} | 0 \rangle \\ &= 0 . \end{aligned} \quad (2.67)$$

As we could guess, without any interactions, there is no way a photon could become a fermion and anti-fermion. To the first order for “ e ”:

$$\begin{aligned}\langle f|U|i\rangle_{\mathcal{O}(e^1)} &= -i\langle 0|c_{p_-}d_{p_+}\left(\int d^4x\mathcal{H}_I\right)a_{p_\gamma}^\dagger|0\rangle \\ &= -i\langle 0|c_{p_-}d_{p_+}\left(\int d^4x(i e)\bar{\psi}A_\mu\gamma^\mu\psi\right)a_{p_\gamma}^\dagger|0\rangle.\end{aligned}\quad (2.68)$$

plugging in our Fourier mode expansion, only the a piece from A_μ and the d^\dagger and c^\dagger piece from the ψ and $\bar{\psi}$ contribute. The other terms will commute and annihilate with $|0\rangle$ or $\langle 0|$. After using our commutator relationships to simplify the contributing terms, we arrive to

$$\begin{aligned}\langle f|U|i\rangle_{\mathcal{O}(1)} &= e\int d^4x(i e)\epsilon_\mu^{s_\gamma}(p_\gamma)\bar{u}_{p_-}^{s_-}\gamma^\mu v_{p_+}^{s_+}e^{-i(p_\gamma-p_- - p_+)\cdot x} \\ &= e(2\pi)^4\delta^4(p_\gamma-p_+-p_-)\epsilon_\mu^{s_\gamma}\bar{u}_{p_-}^{s_-}\gamma^\mu v_{p_+}^{s_+}.\end{aligned}\quad (2.69)$$

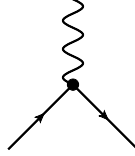
Notice that this result nicely imposes momentum conservation [13]. In QFT, we define an object, called the “scattering amplitude”, \mathcal{M} , such that

$$\langle f|U|i\rangle = (2\pi)^4\delta^4(p_\gamma-p_+-p_-)i\mathcal{M}.\quad (2.70)$$

Therefore for our example,

$$i\mathcal{M} = \epsilon_\mu^{s_\gamma}\bar{u}_{p_-}^{s_-}(-ie\gamma^\mu)v_{p_+}^{s_+}.\quad (2.71)$$

We interpret the $\epsilon_\mu^{s_\gamma}$ term as corresponding to an initial state external photon, $\bar{u}_{p_-}^{s_-}$ as corresponding to a final state external fermion, and $v_{p_+}^{s_+}$ as corresponding to a final state external anti-fermion. We describe $(-ie\gamma^\mu)$ as corresponding to a “vertex interaction”. Graphically, we understand this scattering amplitude to be associated with the *Feynman Diagram*:



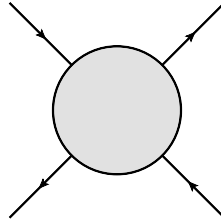
More complex processes in QED will have more and more insertions of the vertex interaction, producing many more Feynman diagrams. This procedure gets systematized by the so-called Feynman rules of QED which we describe next.

2.5 Feynman Diagrams and Feynman Rules

We can now study interactions between fermions and photons. These interactions can be represented with figures known as Feynman Diagrams. It is often easier to construct these graphical representations of an interaction and then recover the corresponding scattering amplitude from the pictures.

2.5.1 Feynman Diagrams

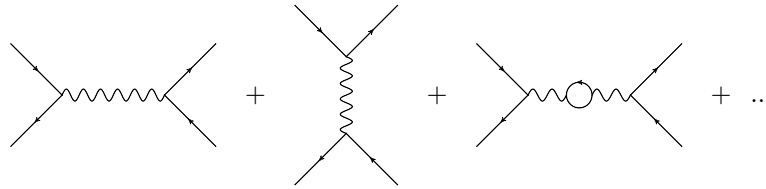
Feynman diagrams are constructed by connecting external initial and final particles. For example, for electron–positron scattering all possible Feynman diagrams can be represented in the diagram below where all possible interactions are enclosed in the circular blob.



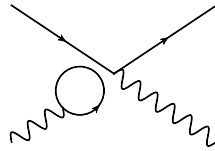
The interactions enclosed in the circular blob follow the following rules:

All:

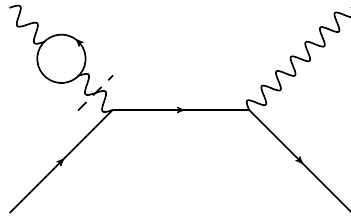
The connection happens in all possible topologically inequivalent manners. For example, the lowest order Feynman diagrams in the series for an electron-positron scattering are presented:

**Connected:**

All external particles are fully connected to one another. Below is an example of a Compton scattering diagram which is *not* fully connected.

**Amputated:**

All interactions that occur with a single external particle such that the external particle is recovered after the interaction is amputated from the diagram. Below is an example of a Compton scattering Feynman diagram which can be amputated at the dotted line.

**2.5.2 QED Feynman Rules for Scattering Amplitudes**

Using the steps above to create Feynman diagrams, we can use the following rules to translate between the pictorial Feynman diagrams to recover the corresponding mathematical expressions that they imply. Below is the list of Feynman rules for QED. Asterisks (*) are included next to Feynman rules which hold for all interactions, QED or otherwise.







Express scattering amplitude:*

$$i\mathcal{M} = \text{sum of all topologically inequivalent, connected, amputated Feynman diagrams.}$$



Symmetry:*

If the graph associated to a Feynman diagram has a symmetry, include $\frac{1}{s}$ where s is the symmetry factor

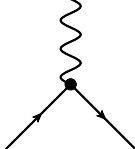
External Wave Functions:

External Fermions		=	$u^s(p)$ initial
		=	$\bar{u}^s(p)$ final
External Anti-Fermions		=	$\bar{v}^s(p)$ initial
		=	$v^s(p)$ final
External Photon		=	$\epsilon_\mu(p)$ initial
		=	$\epsilon_\mu^*(p)$ final

Propagators:

Photon Propagator (Feynman gauge)		=	$\frac{-ig^{\mu\nu}}{p^2+i\epsilon}$
Fermion Propagator		=	$i \frac{\not{p}+m}{p^2-m^2+i\epsilon}$

Vertices:

QED Vertex		=	$-ie\gamma^\mu$
------------	---	---	-----------------

Momentum Conservation:*

Four momentum is conserved at each vertex.

Integrate:*

Integrate over each undetermined “loop” momentum: $\int \frac{d^4 l}{(2\pi)^4}$. These integrals are known as Feynman integrals. The rest of this work is dedicated to the description of a family of one- and two-loop Feynman integrals, and then next we explore some of their properties.

3 Feynman Integrals

Under Feynman rules for quantum field theories, the most general L -loop Feynman integrals can be written in the form,

$$I^{(L)}(\{\rho_1, \dots, \rho_N\}) = \int \frac{d^4 l_1}{(2\pi)^4} \dots \frac{d^4 l_L}{(2\pi)^4} \frac{1}{\rho_1 \rho_2 \dots \rho_N}, \quad (3.1)$$

where $\rho_i = (l' + k')^2 + m^2 - i\epsilon$, with l' being some combination of loop momenta and k' being some combination of external momenta. Notice that Feynman integrals are by construction Lorentz invariant. In general, the computation of these Feynman integrals can be rather cumbersome.

3.1 Dimensional Regularization

Due to divergences when calculating Feynman integrals, of ultraviolet (UV) and infrared (IR) nature we make an analytic continuation in the dimension in which the loop momenta live. That is, instead of working in $D = 4$ dimensions we set $D = 4 - 2\epsilon$ which lets us explore the properties of these integrals for generic ϵ , and only at late stages of calculations we take the limit $\epsilon \rightarrow 0$. This is the *dimensional regularization* (DimReg) method.

In DimReg we write Feynman integrals in the form

$$I(p_1, \dots, p_E; m_1^2, \dots, m_P^2; \nu; D) = \int \left(\prod_{n=1}^L e^{\gamma \epsilon} \frac{d^D k_n}{i\pi^{D/2}} \right) \frac{\mathcal{N}(\{k_i \cdot k_j, k_m \cdot p_k\}; D)}{\prod_{l=1}^P (m_l^2 - q_l^2 - i\epsilon)^{\nu_l}}, \quad (3.2)$$

where L is the number of loops in our Feynman integral, E is the number of external momenta, P is the number of propagators, γ is the Euler–Mascheroni constant, $\nu = (\nu_1, \dots, \nu_P)$ is the vector of propagator powers, D is the dimension of the loop momenta (sometimes written as $D = D_0 - 2\epsilon$), and $\mathcal{N}(\{k_i \cdot k_j, k_m \cdot p_k\}; D)$ represents a general numerator, which will be set by the details of the specific quantum field theory that we consider [3]. Here we define q_i to be a linear combination of external and loop momenta of the form,

$$q_i^\mu = \sum_{j=1}^L \alpha_{ij} k_j^\mu + \sum_{j=1}^{E-1} \beta_{ij} p_j^\mu, \quad (3.3)$$

where α_{ij} and β_{ij} are the constants relating the external and loop momenta to the propagator momenta, which can take to values 0, -1, or 1. We also find it useful to define

$$|\nu| = \sum_{l=1}^P \nu_l. \quad (3.4)$$

Throughout our work, we use the all outgoing convention for momentum and assume that m_l^2 is non-negative for all propagators.

3.1.1 Properties of Feynman Integrals in Dimensional Regularization

From some inherent properties of Feynman integrals and from some consequences of DimReg, we uncover a few useful properties of Feynman Integrals.

Lorentz Invariant

Feynman integrals are Lorentz invariant, meaning that if Λ is a Lorentz transformation

$$I(\Lambda p_1, \dots, \Lambda p_E; m_1^2, \dots, m_P^2; \nu; D) = I(p_1, \dots, p_E; m_1^2, \dots, m_P^2; \nu; D). \quad (3.5)$$

Therefore, we can represent Feynman integrals as a function of a minimal (independent) set of external scalars, which can be built from the Lorentz invariants $\{p_i \cdot p_j\}_{1 \leq i, j \leq E}$ and $\{m_j^2\}_{1 \leq j \leq P}$. We denote such minimal set by \vec{x} .

Associated Graph

Every Feynman integral has an associated graph. These graphs are related to our Feynman Diagrams. This property allows us to apply tools from graph theory when computing Feynman integrals.

Scaling Properties

If we multiply the kinematic scales \vec{x} by some $\lambda \in \mathbb{R}^*$, then

$$\mathcal{N}(\lambda^2 \{k_i \cdot k_j, k_m \cdot p_k\}; D) = \lambda^{\alpha_{\mathcal{N}}} \mathcal{N}(\{k_i \cdot k_j, k_m \cdot p_k\}; D), \quad (3.6)$$

where $\alpha_{\mathcal{N}}$ is the degree of the homogeneous numerator function \mathcal{N} . Therefore,

$$I(\lambda^2 \vec{x}; \nu; D) = \lambda^{\alpha_I} I(\vec{x}; \nu; D), \quad (3.7)$$

where $\alpha_I = \alpha_{\mathcal{N}} + LD - 2|\nu|$.

Scaleless Feynman Integrals

By applying the previous scaling property to some scaleless integral, $I(\vec{0}; \nu; D)$, we conclude that a scaleless Feynman integral in DimReg fulfills:

$$I(\vec{0}; \nu; D) = 0 . \quad (3.8)$$

3.2 Feynman Integral Representations

So far the presentation of Feynman integrals in this document have used a momentum representation (integration is performed in the loop momenta). However, there are multiple ways to express Feynman integrals which give different insights into their properties. Different representations can be easier to handle or it can give different information. Next, we compile some of useful representations for our study.

3.2.1 Momentum Representation

Let's reinstate our definition of Feynman integrals in what is called the momentum representation. This is

$$I(\vec{x}; \nu; D) = \int \left(\prod_{j=1}^L e^{\gamma \epsilon \frac{d^D k_j}{i\pi^{D/2}}} \right) \frac{\mathcal{N}(\{k_i \cdot k_j, k_m \cdot p_k\}; D)}{\prod_{l=1}^P (m_l^2 - q_l^2 - i\epsilon)^{\nu_l}} . \quad (3.9)$$

We repeat the equation here for completeness. We will use this momentum representation to build the other representations we are interested in using.

3.2.2 Schwinger Representation

The first representation we are interested in is called the Schwinger representation. Here we employ *Schwinger's trick* which is the following mathematical relation:

$$\frac{1}{A^\nu} = \frac{1}{\Gamma(\nu)} \int_0^\infty d\alpha \alpha^{\nu-1} e^{-\alpha A} , \quad (3.10)$$

where $\Gamma(\nu)$ is the gamma function given by

$$\Gamma(z) = \int_0^\infty t^{z-1} e^{-t} dt . \quad (3.11)$$

Starting by taking the denominator in the momentum representation, equation (3.9), and applying Schwinger's trick

$$\frac{1}{(-q_j^2 + m_j^2)^{\nu_j}} = \frac{1}{\Gamma(\nu_j)} \int_0^\infty d\alpha_j \alpha_j^{\nu_j-1} \exp(-\alpha_j (-q_j^2 + m_j^2)) , \quad (3.12)$$

where we absorbed the $i\epsilon$ term into the m_j^2 term, we can express the integral as

$$I(\vec{x}; \nu; D) = \frac{e^{L\gamma\epsilon}}{\prod_{j=1}^P \Gamma(\nu_j)} \int_{\alpha_j \geq 0} d^P \alpha \left(\prod_{j=1}^P \alpha_j^{\nu_j-1} \right) \left(\int \prod_{r=1}^L \frac{d^D k_r}{i\pi^{D/2}} \right) \exp \left(\sum_{j=1}^P \alpha_j (-q_j^2 + m_j^2) \right) . \quad (3.13)$$

We now simplify by defining new variables. Taking the exponential term and expanding,

$$\sum_{j=1}^P \alpha_j (-q_j^2 + m_j^2) = - \sum_{r=1}^L \sum_{s=1}^L k_r M_{rs} k_s + \sum_{r=1}^L 2k_r \cdot \bar{\nu}_r + J , \quad (3.14)$$

where M_{rs} is an $L \times L$ matrix with scalar entries, $\bar{\nu}_r$ is a vector with L entries, each one a 4-vector, and J contains scalar terms. We now define

$$\mathcal{U} = \det(M) , \quad (3.15)$$

$$\mathcal{F} = \det(M) (J + \bar{\nu}^T M^{-1} \nu) , \quad (3.16)$$

where \mathcal{U} and \mathcal{F} are called the “graph” polynomials, or the first and second Symanzik polynomials, respectively. We will now show why we have made these definitions. Consider some generic integral T , of the form

$$T = \int dy_1 \dots dy_m \exp(-\vec{y}^T A \vec{y} + 2\vec{w}^T \vec{y} + c) , \quad (3.17)$$

where A is an $m \times m$ symmetric positive-definite matrix, \vec{w} is an m vector, and c is an arbitrary constant. By making the change of variable $\vec{y} = \vec{v} + A^{-1} \vec{w}$,

$$\begin{aligned} T &= \int dv_1 \dots dv_m \exp(-\vec{v}^T A \vec{v}) \exp(\vec{w}^T A^{-1} \vec{w} + c) \\ &= \pi^{m/2} (\det(A))^{-1/2} \exp(\vec{w}^T A^{-1} \vec{w} + c) . \end{aligned} \quad (3.18)$$

Using this in our loop-momenta integral, we arrive at the Schwinger representation:

$$I(\vec{x}; \nu; D) = \frac{e^{L\gamma\epsilon}}{\prod_{j=1}^P \Gamma(\nu_j)} \int_{\alpha_j \geq 0} d^P \alpha \left(\prod_{j=1}^P \alpha_j^{\nu_j-1} \right) \mathcal{U}^{-\frac{D}{2}}(\alpha) \exp\left(\frac{-\mathcal{F}(\alpha; \vec{x})}{\mathcal{U}(\alpha)}\right) . \quad (3.19)$$

This is a P -fold integral as opposed to the $(D \times L)$ -fold integral we had in the momentum representation. Recall that P is the number of propagators in the integral.

3.2.3 Feynman Representation

Building off of the Schwinger representation we can construct another useful Feynman integral representation. From $\sum_{j=1}^P \alpha_j \geq 0$, we can write the identity

$$1 = \int_{-\infty}^{\infty} dt \delta\left(t - \sum_{j=1}^P \alpha_j\right) = \int_0^{\infty} dt \delta\left(t - \sum_{j=1}^P \alpha_j\right) . \quad (3.20)$$

So we can then re-express integrals of functions over $d^P \alpha$ as

$$\int_{\alpha_j \geq 0} d^P \alpha f(\alpha_1, \dots, \alpha_p) = \int_{a_j \geq 0} d^P a \int_0^{\infty} dt \delta\left(t - \sum_{j=1}^P \alpha_j\right) f(\alpha_1, \dots, \alpha_p) . \quad (3.21)$$

Then, by making the change of variables $\frac{\alpha_j}{t} = a_j$,

$$\int_{\alpha_j \geq 0} d^P \alpha f(\alpha_1, \dots, \alpha_p) = \int_{a_j \geq 0} d^P a \delta\left(1 - \sum_{j=1}^P a_j\right) \int_0^{\infty} dt t^{P-1} f(ta_1, \dots, ta_p) . \quad (3.22)$$

Applying this identity to the Schwinger representation we get

$$\begin{aligned} I(\vec{x}; \nu; D) &= \frac{e^{L\gamma\epsilon}}{\prod_{j=1}^P \Gamma(\nu_j)} \int_{a_j \geq 0} d^P a \left(\prod_{j=1}^P a_j^{\nu_j-1} \right) \delta\left(1 - \sum_{j=1}^P a_j\right) \\ &\quad \int_0^{\infty} dt t^{|\nu| + \frac{LD}{2} - 1} \mathcal{U}^{-\frac{D}{2}}(\alpha) \exp\left(\frac{-\mathcal{F}(\alpha; \vec{x})}{\mathcal{U}(\alpha)}\right) . \end{aligned} \quad (3.23)$$

By making a change of variables $t' = \frac{\mathcal{F}}{\mathcal{U}}$

$$I(\vec{x}; \nu; D) = \frac{e^{L\gamma\epsilon}\Gamma(|\nu| - \frac{LD}{2})}{\prod_{j=1}^P \Gamma(\nu_j)} \int_{a_j \geq 0} d^P a \delta \left(1 - \sum_{j \in s} a_j \right) \left(\prod_{j=1}^P a_j^{\nu_j-1} \right) \frac{[\mathcal{U}(a)]^{-|\nu| - \frac{(L+1)D}{2}}}{[\mathcal{F}(a; \vec{x})]^{|\nu| - \frac{LD}{2}}} \int_0^\infty dt' (t')^{v - \frac{LD}{2} - 1} e^{-t'} . \quad (3.24)$$

Then by noticing that the last integral is just $\Gamma(\nu - \frac{LD}{2})$, we obtain

$$I(\vec{x}; \nu; D) = \frac{e^{L\gamma\epsilon}\Gamma(|\nu| - \frac{LD}{2})}{\prod_{j=1}^P \Gamma(\nu_j)} \int_{a_j \geq 0} d^P a \delta \left(1 - \sum_{j \in s} a_j \right) \left(\prod_{j=1}^P a_j^{\nu_j-1} \right) \frac{[\mathcal{U}(a)]^{-|\nu| - \frac{(L+1)D}{2}}}{[\mathcal{F}(a; \vec{x})]^{|\nu| - \frac{LD}{2}}} . \quad (3.25)$$

This is the Feynman representation of the Feynman integral. The parameters a_j are called the Feynman parameters. One of the advantages of this representation is that it makes clear that singularities in the Feynman integral are related to the zeroes of the second Symanzik polynomial $\mathcal{F}(a; \vec{x})$.

3.2.4 Lee-Pomeransky Representation:

For the sake of completion, we present the Lee-Pomeransky Representation of the Feynman integral without derivation.

$$I(\vec{x}; \nu; D) = \frac{e^{L\gamma\epsilon}\Gamma(\frac{D}{2})}{\Gamma(\frac{(L+1)D}{2} - |\nu|) \prod_{j=1}^P \Gamma(\nu_j)} \int_{u_j \geq 0} d^P u \left(\prod_{j=1}^P u_j^{\nu_j-1} \right) [\mathcal{G}(u)]^{-D/2} , \quad (3.26)$$

where

$$\mathcal{G}(\alpha) = \mathcal{U}(\alpha) + \mathcal{F}(\alpha; \vec{x}) . \quad (3.27)$$

This representation is represented by one polynomial \mathcal{G} as opposed to two for the Feynman representation. For a more in depth discussion see [18].

3.2.5 Baikov Representation:

Baikov representation is introduced when a specific requirement is met. Defining

$$e = \dim \langle p_1, p_2, \dots, p_E \rangle . \quad (3.28)$$

Where p_i are external momenta. Whenever $E \leq 5$ we get $e = E - 1$, and other wise $e = 4$.

Let σ be a set of dot products of loop momenta and external momenta,

$$\sigma = \{-k_i^2 | 1 \leq i \leq L\} \cup \{-k_i \cdot k_j | 1 \leq i < j \leq L\} \cup \{-k_i \cdot p_j | 1 \leq i \leq L, 1 \leq j \leq e\} . \quad (3.29)$$

The number of terms in σ , i.e. the number of independent scalar products, is then expressed by,

$$N_\nu = \frac{1}{2}L(L+1) + eL . \quad (3.30)$$

So, we say that a Feynman integral has a Baikov representation if

$$N_\nu = P , \quad (3.31)$$

where P is the number of propagators.

For diagrams which satisfy these conditions we can transform inverse propagators into dot products included in the set σ . Defining

$$z_i = -q_i^2 + m_i^2 , \quad (3.32)$$

we can then find f_i functions, independent of loop momentum, such that

$$z_i = c_{ij}\sigma_j + f_i, \quad \forall i = 1, \dots, P, \quad (3.33)$$

with the matrix c_{ij} invertible by construction. Therefore we can express σ_j as follows,

$$\sigma_j = (c^{-1})_{ji} (z_i + f_i). \quad (3.34)$$

This allows us to make a change of variables between in the momentum representation integral, from the k_j with $j = 1, \dots, L$, to the z_i . By employing this change of variables we obtain the Baikov representation,

$$I(\vec{x}; \nu; D) = \frac{e^{L\gamma\epsilon} [\det(G(p_1 \dots p_e))]^{-(D+e+1)/2}}{\pi^{\frac{1}{2}(N_\nu-L)} (\det(\mathcal{C})) \prod_{j=1}^P \Gamma\left(\frac{D-e+1+j}{2}\right)} \int_{\mathcal{C}} d^{N_\nu} z \frac{[B(z)]^{\frac{D-l-e-1}{2}}}{\prod_{s=1}^{N_\nu} z_s^{-\nu_s}}, \quad (3.35)$$

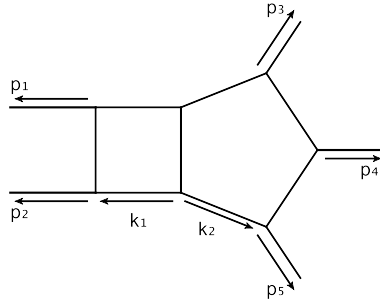
where \mathcal{C} is some non-trivial contour, $G(q_1, \dots, q_m)_{i,j} = -q_i \cdot q_j$, and $B(z) = B(z_1, \dots, z_{N_\nu}) = \det[G(k_1, \dots, k_L, p_1, \dots, p_e)]$, known as the Baikov polynomial. The Baikov representation naturally let's us take the “cut” of a Feynman integral, that is the residue when the inverse propagators $-q_i^2 + m_i^2$ go “on-shell”, that is, when they go to zero. This operation is essential for modern techniques to compute Feynman integrals, for example when building their corresponding differential equations, or in the so-called numerical unitary method which we outline in section 5.

Irreducible Scalar Products

Recall how we mentioned that in order to express a Feynman integral in the Baikov Representation we require that $N_\nu = P$, however, even if $N_\nu > P$ we can still “complete” the corresponding propagator structure by introducing propagators not originally present. Those extra propagators are related to scalar products involving loop momentum which are not connected to existing propagators. We call those scalar products *irreducible* scalar products (ISPs). To make this more concrete we explore a two-loop example.

Pentabox Example

The so-called pentabox two-loop Feynman integral provides a clear example of building a complete Feynman integral from ISPs. This integral is specified by the following graph.



Counting the propagators, we see that $P = 8$. However, looking at the dot products involving loop momentum, $N_\nu = 11$,

$$\sigma = \{-k_1^2, -k_2^2, -k_1 \cdot k_2, -k_1 \cdot p_2, -k_1 \cdot p_3, -k_1 \cdot p_4, -k_1 \cdot p_5, -k_2 \cdot p_2, -k_2 \cdot p_3, -k_2 \cdot p_4, -k_2 \cdot p_5\}$$

seven of these are easily able to be related to propagators in the diagram, leaving four scalar products of interest,

$$\{-k_1 \cdot p_3, -k_1 \cdot p_4, -k_1 \cdot p_5, -k_2 \cdot p_2\}.$$

Note that one of these scalar products are able to be reduced to expressions of other scalar products,

$$\begin{aligned} k_1 \cdot (p_3 + p_4 + p_5) &= -k_1 \cdot (p_1 + p_2) \\ \Rightarrow k_1 \cdot p_3 &= -k_1 \cdot (p_1 + p_2 + p_4 + p_5) \end{aligned}$$

Thus we can reduce $-k_1 \cdot p_3$ using the propagator between p_1 and p_2 , $-k_1 \cdot p_4$, and $-k_1 \cdot p_5$. In order to keep $-k_1 \cdot p_3$ we must take $-k_1 \cdot p_4$ and $-k_1 \cdot p_5$ to be irreducible. We cannot reproduce this reduction with $-k_2 \cdot p_2$ because there is not a propagator allowing this procedure already in our diagram. Thus we have three irreducible scalar products for the pentabox,

$$\{-k_1 \cdot p_4, -k_1 \cdot p_5, -k_2 \cdot p_2\}.$$

Now, we “enlarge” our Feynman diagram by introducing propagators corresponding to these ISPs,

$$\begin{aligned}\rho_9 &= (-k_1 + p_4)^2, \\ \rho_{10} &= (-k_1 + p_5)^2, \\ \rho_{11} &= (-k_2 + p_2)^2.\end{aligned}$$

This allows us to write our Feynman integral for this diagram in the following manner,

$$I(\vec{x}; \nu; D) = \int \left(\prod_{j=1}^L e^{\gamma \epsilon} \frac{d^D k_j}{i\pi^{D/2}} \right) \frac{1}{\left(\prod_{l=1}^P (m_l^2 - q_l^2 - i\epsilon)^{\nu_l} \right) \rho_9^{\nu_9} \rho_{10}^{\nu_{10}} \rho_{11}^{\nu_{11}}},$$

which we have shown in the momentum representation to make the propagators explicit. We can recover our original integral family¹ by setting $\nu_9 = \nu_{10} = \nu_{11} = 0$. However, with this complete family for the pentabox we can represent the pentabox Feynman integral in the Baikov representation. Thus we can take cuts for the pentabox (where all but the ISP propagator go to zero). This procedure is very important for our study our main integral of interest, the double box.

3.3 Integration By Parts Relations

For a generic Feynman integral $I(\vec{x}; \nu; D)$, in dimensional regularization if $|\nu| = \sum_{j=1}^P \nu_j \leq 0$ then $I = 0$. For a fixed \vec{x} , there are relationships between $I(\vec{x}; \nu; D)$, such that there are only a finite number of linearly independent Feynman integrals. The minimum linearly independent set of Feynman integrals are called the *master integrals*.

In dimensional regularization

$$\int \frac{d^D k_j}{(i\pi^{D/2})} \frac{\partial}{\partial k_j^\mu} (\nu^\mu F_I(k_1, \dots, k_L; p_1, \dots, p_P; \nu; D)) = 0, \quad (3.36)$$

where ν^μ is a generic D -dimensional vector and $F_I(k_1, \dots, k_L; p_1, \dots, p_P; \nu; D)$ is the integrand of a Feynman integral, that is

$$F_I(k_1, \dots, k_L; p_1, \dots, p_P; \nu; D) = \frac{\mathcal{N}(\{k_i \cdot k_j, k_i \cdot p_j\}; D)}{\prod_{j=1}^P (m_l^2 - q_l^2)^{\nu_j}}.$$

Using this, we consider $\frac{\partial}{\partial k_i^\mu}$ acting on $\frac{1}{(m_j^2 - q_j^2)^{\nu_j}}$. For example, if $q_j = k_i + p_1$, where p_1 is an external momentum, consider

$$\frac{\partial}{\partial k_i^\mu} \left(\frac{\nu^\mu}{(m_j^2 - q_j^2)^{\nu_j}} \right), \quad (3.37)$$

where ν^μ is independent of k_i^μ . Therefore,

$$\frac{\partial}{\partial k_i^\mu} \left(\frac{\nu^\mu}{(m_j^2 - q_j^2)^{\nu_j}} \right) = \frac{\nu^\mu}{(m_j^2 - q_j^2)^{\nu_j+1}} \nu_j 2(k_{i\mu} + p_{1\mu}). \quad (3.38)$$

¹We define an *integral family* as the set of all Feynman integrals which share a common propagator structure.

Choosing $\nu^\mu = p_1^\mu$,

$$\begin{aligned} \frac{\partial}{\partial k_i^\mu} \left(\frac{\nu^\mu}{(m_j^2 - q_j^2)^{\nu_j}} \right) &= \frac{2\nu_j}{(m_j^2 - q_j^2)^{\nu_j+1}} p_1 (k_i + p_1) \\ &= \frac{\nu_j \left((k_i + p_1)^2 - k_i^2 + p_1^2 \right)}{(m_j^2 - q_j^2)^{\nu_j+1}} . \end{aligned} \quad (3.39)$$

Say $q_1^2 = k_i^2$,

$$\frac{\partial}{\partial k_i^\mu} \left(\frac{\nu^\mu}{(m_j^2 - q_j^2)^{\nu_j}} \right) = \frac{\nu_j \{ (m_1^2 - q_1^2) - (m_j^2 - q_j^2) + (p_1^2 - m_1^2 + m_j^2) \}}{(m_j^2 - q_j^2)^{\nu_j+1}} . \quad (3.40)$$

Expanding this term and simplifying, we can then use equation (3.36) to conclude that

$$\int \frac{d^D k_j}{(i\pi^{D/2})^{\nu_j}} \left[-\frac{1}{(m_j^2 - q_j^2)^{\nu_j}} + \frac{1}{(m_1^2 - q_1^2)^{-1} (m_j^2 - q_j^2)^{\nu_j+1}} + \frac{p_1^2 - m_1^2 + m_j^2}{(m_j^2 - q_j^2)^{\nu_j+1}} \right] = 0 . \quad (3.41)$$

This specific example shows that the total derivative acting on an integrand provides us with relationships between integrals in the same family. This helps us reduce the number of integrals that we actually have to calculate when a family of Feynman integrals contains a large number of integrals.

Formally, every complete family of Feynman Integrals satisfies linear recursion relations in the propagator exponents $\nu \in \mathbb{Z}^P$, which are called integration-by-parts (IBP) identities. The coefficients of the linear combinations are rational functions in the external scales \vec{x} and in the dimensional regulator $\epsilon(D)$. The number of master integrals is finite for every family of Feynman integrals [16] [6].

3.3.1 IBP Example: One-Loop bubble

To help understand IBP relations, here we cover the example of a one-loop bubble, which has the Integral

$$I(p^2; m_1^2; m_2^2; \nu_1, \nu_2, D) = e^{\gamma\epsilon} \int \frac{d^D k}{i\pi^{D/2}} \frac{1}{(m_1^2 - k^2)^{\nu_1} (m_2^2 - (k-p)^2)^{\nu_2}} . \quad (3.42)$$

More specifically, we will look at the special case where $m_1^2 = m_2^2 = 0$. In this case if $\nu_1 \leq 0$ or $\nu_2 \leq 0$, then $I(\nu_1, \nu_2) = 0$. So to find IBP relations we take

$$\int \frac{d^D k}{(i\pi^{D/2})} \frac{\partial}{\partial k^\mu} \left(\nu^\mu \frac{1}{(-q_1^2)^{\nu_1} (-q_2^2)^{\nu_2}} \right) = 0 , \quad (3.43)$$

where $-q_1^2 = -k^2$ and $-q_2^2 = -(k-p)^2$. If set $\nu^\mu = k^\mu$, we get the first IBP relationship

$$(D - 2\nu_1 - \nu_2) I(\nu_1, \nu_2) - \nu_2 I(\nu_1 - 1, \nu_2 + 1) - \nu_2 p^2 I(\nu_1, \nu_2 + 1) = 0 . \quad (3.44)$$

As we would prefer to set ν_1 and $\nu_2 \leq 0$, we redefine $(\nu_2 + 1) \rightarrow \nu_2$ (restricting us to using this IBP relationship only for $\nu_2 \neq 1$) so that we can rewrite equation (3.44) into

$$I(\nu_1, \nu_2) = \frac{D + 1 - 2\nu_1 - \nu_2}{p^2 (\nu_2 - 1)} I(\nu_1, \nu_2 - 1) - \frac{1}{p^2} I(\nu_1 - 1, \nu_2) . \quad (3.45)$$

We can get a second IBP relation by setting $\nu^\mu = p^\mu$, this gives

$$\begin{aligned} (\nu_1 - \nu_2) I(\nu_1, \nu_2) - \nu_1 I(\nu_1 + 1, \nu_2 - 1) - \nu_1 p^2 I(\nu_1 + 1, \nu_2) \\ + \nu_2 I(\nu_1 - 1, \nu_2 + 1) + \nu_2 p^2 I(\nu_1, \nu_2 + 1) = 0 . \end{aligned} \quad (3.46)$$

Using the first IBP relationship, equation (3.44), we see that we can simplify the last two terms. Additionally, we can see that we should redefine $(\nu_1 + 1) \rightarrow \nu_1$ (restricting us to using this IBP relationship only for $\nu_1 \neq 1$). This gives the simplified form of the second IBP relation

$$I(\nu_1, \nu_2) = \frac{D+1-2\nu_2-\nu_1}{p^2(\nu_1-1)} I(\nu_1-1, \nu_2) - \frac{1}{p^2} I(\nu_1, \nu_2-1) . \quad (3.47)$$

With these two IBP relationships, we find that the complete family $I(\nu_1, \nu_2)$ has a single master integral, which we can choose to be $I(1, 1)$. This integral can be computed and gives:

$$I(1, 1) = e^{\gamma\epsilon} (-p^2)^{\frac{D-4}{2}} \frac{\Gamma(2 - \frac{D}{2}) \Gamma(\frac{D}{2} - 1)^2}{\Gamma(D-2)} . \quad (3.48)$$

This means that all we have to do to solve for any $I(\nu_1, \nu_2)$ is use the two IBP relationships, equation (3.45) and (3.46), to solve for the rational coefficient of then master integral $I(1, 1)$, drastically reducing the complexity of the problem.

As demonstrated, IBP relations are a powerful tool for calculating Feynman integrals, especially those of greater complexities. This is one of the main techniques we use in this research, and it is vital for calculating the Feynman diagrams that we will study.

4 Einstein Hilbert Gravity

For Gravitational wave astronomy, we are interested in the potential between bound binary systems, such as binary black holes. To solve for this we can use the techniques we learned from QFT and apply them to an effective field theory of weak gravity on scalar particles. Similar to how we modeled interactions between the photon, the carrier of the electromagnetic force, and charged fermions, we can model the interactions between a hypothetical gravitational force carrier, the graviton, and a scalar particle, such as a black hole. Even though these bound systems do not scatter, the potential between an open scattering system and a bound system are related, so we can consider scattering black holes to calculate their bound potential.

To do this we need a Lagrangian for gravity, called the Einstein-Hilbert Lagrangian.:

$$\mathcal{L}_{EH} = -\frac{2}{\kappa^2} \sqrt{|g|} R , \quad (4.1)$$

or for a scalar field theory interacting through gravity

$$\mathcal{L} = \sqrt{-g} \left[-\frac{2R}{\kappa^2} + \frac{1}{2} g^{\mu\nu} \partial_\mu \phi \partial_\nu \phi - \frac{1}{2} m^2 \phi^2 + \dots \right] , \quad (4.2)$$

where $\kappa = \sqrt{32\pi G}$, G is Newton's constant, $g_{\mu\nu}$ is the metric tensor, $g = \det(g_{\mu\nu})$, and R is the Ricci scalar associated to the curvature of spacetime (see e.g. [11]). In the weak field approximation $g_{\mu\nu} = \eta_{\mu\nu} + \kappa h_{\mu\nu}$, where $h_{\mu\nu}$ is the graviton field [11]. Here we do not consider any other interactions, for example those of electromagnetic nature.

4.1 Feynman Rules for Einstein-Hilbert Gravity

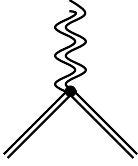
In a similar manner to how we derived the Feynman rules for QED, we can derive Feynman rules from the Lagrangian for our theory of gravity. This process is fully explained in *EPFL Lectures on General Relativity as a Quantum Field Theory* by John F. Donoghue, Mikhail M. Ivanov, and Andrey Shkerin [9]; however, here we just quote the main results.

Propagators:

Graviton Propagator  = $\frac{i P^{\alpha\beta\gamma\delta}}{q^2}$,

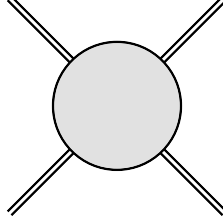
where $P^{\alpha\beta\gamma\delta} = \frac{1}{2} [\eta^{\alpha\gamma} \eta^{\beta\delta} + \eta^{\alpha\delta} \eta^{\beta\gamma} - \eta^{\alpha\beta} \eta^{\gamma\delta}]$.

Vertices:

Graviton Vertex  $= i \frac{\kappa}{2} [(p_\mu p'_\nu + p'_\mu p_\nu) - \eta_{\mu\nu} (p \cdot p' - m^2)]$.

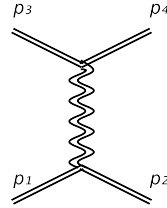
where p_μ and p'_ν are the four momentum of the massive scalar particle. There is an additional three graviton vertex; however, we do not include it in this document for brevity.

Using these Feynman rules we can analyze binary black hole scattering.



4.2 Tree Level Graviton Scattering

Following the derivation in Donoghue [9], for the lowest order (“tree-level”) interaction, we have the Feynman diagram



$$= i\mathcal{M} = \frac{i\kappa}{2} [(p_1^\mu p_2^\nu + p_2^\mu p_1^\nu) - \eta^{\mu\nu} (p_1 \cdot p_2 - m^2)]$$

$$\times \frac{i}{q^2} P_{\mu\nu\alpha\beta} \frac{i\kappa}{2} [(p_3^\alpha p_4^\beta + p_4^\alpha p_3^\beta) - \eta^{\alpha\beta} (p_3 \cdot p_4 - m^2)] .$$
(4.3)

In the non-relativistic static limit $p_i^\mu \approx (m_i, \vec{0})$, so

$$\mathcal{M} = -\frac{\kappa^2}{2} \frac{m_1^2 m_2^2}{q^2} = -16\pi G \frac{m_1^2 m_2^2}{q^2} .$$
(4.4)

The Fourier-transform of \mathcal{M} from momentum space to real space gives us the interaction potential. For this example,

$$V(r) = -\frac{Gm_1 m_2}{r},$$
(4.5)

which is what we would have expected, that is we obtain Newton’s potential (see a more detailed discussion in [9]). As we calculate higher-order corrections to the scattering amplitude \mathcal{M} (by evaluating higher-loop Feynman diagrams), we can calculate relativistic corrections (either in velocity or in Newton’s constant G) to this potential. This allows to calculate the most accurate gravitational potentials to date, surpassing results obtained by standard general relativity methods (for a recent review on this progress, see [7]).

5 Numerical Unitary Method and Integrand Parameterization

In this section we outline a method to obtain numerical results for the amplitude integrand of general scattering processes. First we explore the so-called *cut-equation* which provides a method to break

apart the integrands of Feynman diagrams into a basis of functions, such that we only have to calculate a few integrand coefficients to obtain the amplitude. The rest of the integrands evaluate to zero, we call them *surface terms*, therefore dropping from the amplitude. We will introduce the helpful *adaptive loop parametrization* which provides a representation of loop momenta that can be employed to express the integrand for scattering amplitudes. Then, we outline how this adaptive parametrization is used to construct three integrand bases, which each build on the last to produce more surface terms, progressively simplifying the procedure to compute amplitudes. Obtaining these bases and the coefficients relating the terms in our basis to the amplitude integrand, is the key goal of this research.

5.1 Cut-Equation

We start with the Ansatz that the scattering amplitude can be written as a linear combination of master integrals,

$$\mathcal{A} = \sum_{\Gamma \in \Delta} \sum_{i \in M_\Gamma} c_{\Gamma,i} \mathcal{I}_{\Gamma,i} \quad (5.1)$$

Where M_Γ denotes the set of master integrals, Δ denotes all possible propagator structures of the amplitude, Γ (which we call the *diagram*) is a specific propagator structure $\{\rho_1, \dots, \rho_p\} \in \Delta$ with $\rho_j = m_j^2 - q_j^2 - i\epsilon$, and with q_j corresponding to the momentum of the propagator ρ_j . The coefficients $c_{\Gamma,i}$ are function of $p_i \cdot p_j$ and D . From equation (5.1) we obtain that for generic integrands of scattering amplitudes,

$$\mathcal{A}(\ell_l) = \sum_{\Gamma \in \Delta} \sum_{i \in Q_\Gamma} \frac{c_{\Gamma,i} m_{\Gamma,i}(\ell_l^\Gamma)}{\prod_{j \in P_\Gamma} \rho_j(\ell_l^\Gamma)} \quad (5.2)$$

where ℓ_l represent the loop momenta, Q_Γ is the set containing all master (M_Γ) and surface (S_Γ) functions, and $\{m_{\Gamma,i}\}$ is a set of functions which depend on external momenta, loop momenta, and the dimension of spacetime [2]. It is important to note that $\{m_{\Gamma,i}\}$ is dependent on the propagator structure, but that the propagators are explicitly removed from them.

In the end, we will need to extract the coefficients $c_{\Gamma,i}$. To accomplish this we put our loop-momenta on-shell, that is we choose loop-momenta ℓ_l^Γ such that $\rho_j(\ell_l^\Gamma) = 0$ for all propagators in Γ . In this limit we take only the most singular contribution to the amplitude's integrand (see e.g. [15]). To accomplish this, we take the ansatz (5.2) for some $\Gamma \in \Delta$ and multiply both sides of the equation by the product of the $\rho_j(\ell_l)$ in Γ , then take the limit as all $\rho_j(\ell_l)$ approach zero (that is, when $\ell_l \rightarrow \ell_l^\Gamma$),

$$\lim_{\rho_i \rightarrow 0} \left(\mathcal{A}(\ell_l) \prod_{i \in \Gamma} \rho_i \right) = \lim_{\rho_i \rightarrow 0} \left(\sum_{\Gamma' \in \Delta} \sum_{i \in Q_{\Gamma'}} \frac{c_{\Gamma',i} m_{\Gamma',i}(\ell_l^{\Gamma'})}{\prod_{j \in P_{\Gamma'}} \rho_j(\ell_l^{\Gamma'})} \prod_{i \in \Gamma} \rho_i \right). \quad (5.3)$$

In this limit, we notice that for a generic diagram Γ' with less propagators than Γ , the corresponding integrand will go to zero. On the other hand, Γ' with more propagators than Γ will be non-zero. This implies that there is an ordering, or *hierarchy*, of diagrams in Δ . Some propagator structures have more propagators (the *parents*) than others (the *daughters*). The hierarchy of diagrams for the gravity two-loop amplitude which we are studying is shown in Figure 2.

Note that in the on-shell limit, only the corresponding most-singular contributions survive. Notably, the amplitude's integrand factorizes into a product of tree-level amplitudes. Thus, we are left with the following equation,

$$\sum_{\text{states}} \prod_{i \in T_\Gamma} \mathcal{A}_i^{\text{tree}}(\ell_l^\Gamma) = \sum_{\substack{\Gamma' \geq \Gamma \\ k \in Q_{\Gamma'}}} \frac{c_{\Gamma',k} m_{\Gamma',k}(\ell_l^\Gamma)}{\prod_{j \in (P_{\Gamma'} / P_\Gamma)} \rho_j(\ell_l^\Gamma)}, \quad (5.4)$$

which is known as the *cut-equation*. Here $\mathcal{A}_i^{\text{tree}}$ is the tree level amplitude of each vertex in the diagram Γ and T_Γ correspond to all the vertices in it [8, 15]. As the coefficients $c_{\Gamma',k}$ are only depend on the external variables, sampling the cut equation over multiple values of on-shell loop-momenta ℓ_l^Γ produces systems of linear equations. These linear equations can be solved numerically, and from their solutions we obtain the coefficients! To compute the products of tree-level amplitudes, which are commonly called *the cuts*, we employ the software package called `Caravel`.

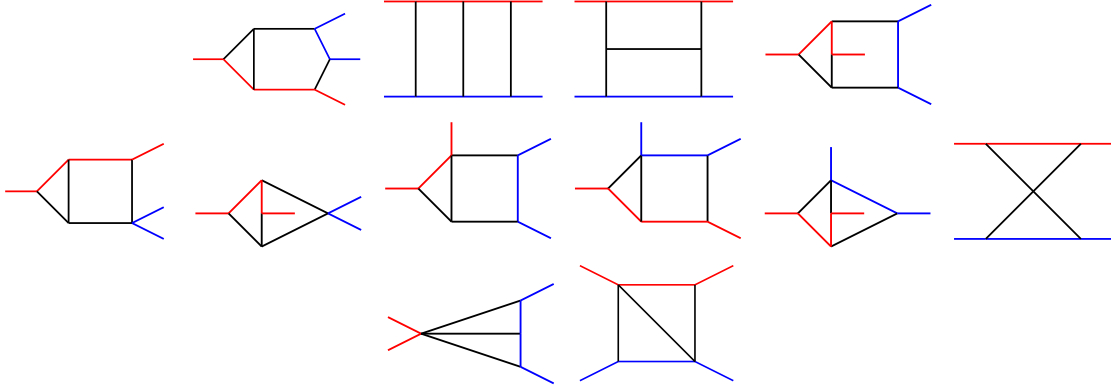


Figure 2: Hierarchy of diagrams for the gravity two-loop amplitude studied in [11]. The blue and red lines represent separate massive particles and the black lines represent massless graviton exchanges. In this work we focus on the diagram that appears second to the left in the top row, the double box.

The Caravel Framework

Caravel [1] is a program that, among other things, produces numerical evaluations for *cuts*, that are products of tree-level amplitudes. **Caravel** accomplishes this over different numerical values of the on-shell loop momenta, essentially using efficient techniques to handle the Feynman rules for the theory presented in section 4. **Caravel** performs numerical calculations using finite field arithmetic to allow for exact calculations. For more details on this program see the release article [1]. With these numerical evaluations in hand, once we obtain a set of basis functions to represent the integrand, we can obtain the corresponding integrand coefficients. We can obtain these set of basis functions using the so-called adaptive loop-momentum parametrizations, as described in the following subsection.

5.2 Adaptive Loop-Momentum Parametrizations

We start working by example. We first consider one-loop diagrams, and use the so-called van Neerven-Vermaseren basis. The extension of it to multi-loop diagrams is what we will call as the *adaptive loop-momentum* parametrization. We follow closely the presentations of [10] (at one-loop level) and of [15] (for multi-loop level).

The loop momentum of a one-loop Feynman integral can be expressed as a linear combination of the following set of vectors:

1. 4-vectors which lie in the space spanned by the external momenta of the diagram, and which have dimension D^p . We call this the *scattering plane* of the diagram.
2. 4-vectors (living within the 4-dimensional Minkowski space) which are transverse to the scattering plane, and which have dimension D^t . Naturally, $4 = D^p + D^t$.
3. vectors which cover extra-dimensional degrees of freedom, as needed in dimensional regularization. We denote the dimensionality of this space as D^ϵ .

We will treat each in turn.

First, for the vectors which lie in the scattering plane, we choose a basis v_i ($i = 1, \dots, D^p - 1$) which satisfy,

$$v_i \cdot p_j = \delta_{ij} , \quad (5.5)$$

where the p_j 's are the external momenta to the one-loop diagram. It is easy to construct such v_i 's by using the Gram matrix

$$G_{ij} = p_i \cdot p_j \quad \text{with} \quad i, j = 1, \dots, D^p - 1 . \quad (5.6)$$

Indeed, we define

$$v_i^\mu = (G^{-1})_{ij} p_j^\mu. \quad (5.7)$$

Now with a set of basis vectors which span the same physical space as our external momenta, we can now consider the set of basis vectors which are transverse to our loop momenta. In our scattering process of interest we have four external momenta, of which only three are linearly independent due to momentum conservation (that is, for us $D^p = 3$). Therefore, we need another vector ($D^t = 1$) which is transverse to our external momenta such that we have the required vectors to span the full 4-dimensional Minkowski space. By construction this transverse vector n_1 obeys the following conditions:

$$\begin{aligned} n_1 \cdot p_j &= 0, \\ n_1 \cdot v_j &= 0, \\ n_1 \cdot n_1 &= 1. \end{aligned} \quad (5.8)$$

We see that for our problem these conditions are satisfied when we define

$$\begin{aligned} \tilde{n}_1^\mu &= \epsilon^{\mu\nu\rho\sigma} p_{1\nu} p_{2\rho} p_{3\sigma}, \\ n_1^\mu &= \frac{\tilde{n}_1^\mu}{|\tilde{n}_1|^2}. \end{aligned} \quad (5.9)$$

Lastly, we must consider the extra dimensional degrees of freedom from dimensional regularization. For this we want a set of extra-dimensional vectors which are orthogonal to our previous vectors, which is easily done by setting all of the 4-dimensional components to 0, and orthogonal to one another, which if we start with random linearly-independent extra-dimensional vectors, can be accomplished using the Gram-Schmidt procedure. The extra-dimensional vectors n_i^ϵ obey the relations:

$$\begin{aligned} n_i^\epsilon \cdot p_j &= 0, \\ n_i^\epsilon \cdot v_j &= 0, \\ n_i^\epsilon \cdot n_j &= 0, \\ n_i^\epsilon \cdot n_j^\epsilon &= \delta_{ij}. \end{aligned} \quad (5.10)$$

With these definitions laid out, we write the loop momentum as

$$\ell = \sum_{j=1}^{D^p} v_j r_j + \sum_{i=1}^{D^t} n_i \alpha_{ct,i} + \sum_{i=1}^{D^\epsilon} n_i^\epsilon \mu_i. \quad (5.11)$$

This is known as the van Neerven-Vermaseren loop-momentum parametrization. Notice that for completeness we have included a sum for the transverse vectors n_i , even though before we worked in an example where there was a single vector n_1 . We can obtain the coefficients of this parametrization using the properties from equations (5.5), (5.8), and (5.10). Doing so we obtain:

$$\begin{aligned} r_j &= p_j \cdot \ell, \\ \alpha_{ct,i} &= n_i \cdot \ell, \\ \mu_i &= n_i^\epsilon \cdot \ell. \end{aligned} \quad (5.12)$$

For multi-loop diagrams we extend this parametrization by noting that the loop momentum may not necessarily encounter all the external momenta in its routing withing the diagram. This happens explicitly for example in the double box which we study. When discussing the van Neerven-Vermaseren loop momentum parametrization we ended up denoting the transverse space variables $\alpha_{ct,i}$ with the letters *ct*. This is because, in the case of multi-loop diagrams there are vectors which are transverse for only a specific loop momentum but not for all loop momenta in the diagram. For a loop momentum in a multi-loop diagram, our vectors v_i^j , corresponding to the unencountered external momenta, act as a transverse vector for the external momenta specific to such loop momentum. The transverse vector that we defined for the one-loop case on the other hand remains common to all external momenta in the diagram. This then is the adaptive loop parametrization.

To write the loop momenta parametrization we introduce the following set of indices: B_l^p the scattering plane for the loop momentum ℓ_l (associated to the basis vectors v_l^i); B_l^t the complement momenta within the scattering plane which is transverse to B_l^p (associated to the basis vectors v_l^j); B^{ct} for the common-transverse space (associated to the basis vectors n^i); and finally B^ϵ for the extra-dimensional space (associated to the basis vectors n_ϵ^i). With this, we then write:

$$\ell_l = \sum_{i \in B_l^p} v_l^i r^{lj} + \sum_{j \in B_l^t} v_l^j \alpha_t^{lj} + \sum_{i \in B^{ct}} n^i \alpha_{ct}^{li} + \sum_{i \in B^\epsilon} n_\epsilon^i \mu_l^i . \quad (5.13)$$

with α_t^{lj} being the coefficient corresponding to the transverse vector for that loop momenta and to the irreducible scalar products (ISPs) discussed in section 3.2.5. We can use this parametrization to obtain the desired set of integrand functions, $\{m_{\Gamma,i}\}$ (see equation (5.2)). In the following sections we will explore three different bases of functions $\{m_{\Gamma,i}\}$.

5.3 Tensor Basis

We start building a basis $\{m_{\Gamma,i}\}$ which is completely independent of the inverse propagators in Γ . We note that we can express both r^{lj} and μ_l^i in terms of propagators. For r^{lj} we note that $p_j \cdot \ell_l$ can be found in the cross term of the propagators as each propagator term is expressed as the square of a linear combination of external momentum p_j and ℓ_l . Thus, r^{lj} can always be re-written in terms of propagator variables,

$$r^{lj} = -\frac{1}{2} \left(\rho_{li} - (q_{li})^2 - \rho_{l(i-1)} + (q_{l(i-1)})^2 \right), \quad (5.14)$$

where q_{li} are combinations of external momenta. With this, we note that a $\mathcal{N}(\{k_i \cdot k_j; k_i \cdot p_m\}; D)$ for a diagram Γ can be expressed in terms of μ_l^i , α_t^{lj} , and α_{ct}^{li} . Everything else will contain inverse propagators ρ_{li} which will cancel with the propagators in the ansatz (5.2). Such terms can be caught by the numerators of daughter diagrams $\Gamma' < \Gamma$.

Considering the propagator which our loop momentum lie on, say ρ_{l1} , we can express the extra-dimensional variable μ_l^i in the following manner,

$$\begin{aligned} \rho_{l1} = \ell_l^2 &= f(r^{lj}, \alpha_t^{lj}, \alpha_{ct}^{li}) + (\mu_l^i)^2 \\ \Rightarrow (\mu_l^i)^2 &= \rho_{l1} - f(r^{lj}, \alpha_t^{lj}, \alpha_{ct}^{li}) . \end{aligned}$$

With these two expressions, since α_t^{lj} and α_{ct}^{li} are the only variables independent of propagators, we can express a generic integrand numerator in terms of monomials built from α_t^{lj} and α_{ct}^{li} ². Therefore, we can represent the numerators of our integrand to be linear combinations of numerators of the form,

$$(\alpha_t^{lj})^{\vec{a}} (\alpha_{ct}^{li})^{\vec{b}}, \quad (5.15)$$

where the exponents are vectors of integers. The collection of these monomials form what we call the tensor basis.

5.4 Scattering-Plane Tensor Basis

Now that we have laid out the form of our tensor basis, we now wish to make a change of basis in a way that we can group basis functions into two sets, M_Γ and S_Γ , such that:

$$\begin{cases} \int d\alpha(\dots) \frac{m_{\Gamma,i}(\{k_i \cdot k_j; k_i \cdot p_m\}; D)}{\rho_1 \dots \rho_p} = I_{\Gamma,i} & i \in M_\Gamma , \\ \int d\alpha(\dots) \frac{m_{\Gamma,i}(\{k_i \cdot k_j; k_i \cdot p_m\}; D)}{\rho_1 \dots \rho_p} = 0 & i \in S_\Gamma . \end{cases} \quad (5.16)$$

Here the $I_{\Gamma,i}$ are master integrals. Such a choice would be convenient as the map from the integrand $\mathcal{A}(\ell_l)$ to the actual (integrated) amplitude \mathcal{A} gets simplified.

²Monomials because in field theory all numerators are polynomial functions of scalar products.

To accomplish this, we first note that monomials with odd powers of (α_{ct}^{li}) integrate to zero because the interval of integration (basically from minus infinity to infinity) is symmetric, i.e.

$$\int d\alpha(\dots) \frac{(\alpha_{ct}^{li})^{(2n-1)}}{\rho_1 \dots \rho_N} = 0, \quad n = 1, 2, 3, \dots \quad (5.17)$$

Here we ignore other integrals needed for full integration for visual clarity.

We can also transform monomials with even powers of (α_{ct}^{li}) to integrate to zero. We will demonstrate this for monomials with $(\alpha_{ct}^{li})^2$ and $(\alpha_{ct}^{li})^4$, the only two which will be relevant for the calculations performed in this study. For notational simplicity we will simply write α_{ct} in the following, and drop other indices and terms that might appear in the integrals.

For the case of $(\alpha_{ct})^2$ we start by using the definition of (α_{ct}) to express our integrand in terms of loop tensor integrals. Once we do this we can use the fact that the result of such integral must be dependent on external loop momentum and metric tensors to write a generic result. This is:

$$\begin{aligned} \int d\alpha(\dots) \frac{\alpha_{ct}^2}{\rho_1 \dots \rho_N} &= n_\mu n_\nu \int d\alpha(\dots) \frac{\ell^\mu \ell^\nu}{\rho_1 \dots \rho_N}, \\ \int d\alpha(\dots) \frac{\ell^\mu \ell^\nu}{\rho_1 \dots \rho_N} &= A g^{\mu\nu} + B q^\mu q^\nu. \end{aligned}$$

From this we can use our definitions our definitions of (α_{ct}) , together with the object $\mu^2 = g_{\mu\nu}^{[D-4]} \ell^\mu \ell^\nu$, to find expressions which are both proportional to the coefficient A in the last equation,

$$\begin{cases} n_\mu n_\nu \int d\alpha(\dots) \frac{\ell^\mu \ell^\nu}{\rho_1 \dots \rho_N} = \int d\alpha(\dots) \frac{\alpha_{ct}^2}{\rho_1 \dots \rho_N} = A, \\ g_{\mu\nu}^{[D-4]} \int d\alpha(\dots) \frac{\ell^\mu \ell^\nu}{\rho_1 \dots \rho_N} = \int d\alpha(\dots) \frac{\mu^2}{\rho_1 \dots \rho_N} = (D-4)A. \end{cases}$$

We have used $g_{\mu\nu}^{[D-4]}$ as the metric tensor in D dimensions subtracted by the metric tensor in 4 dimensions. Using these last two relations, we obtain,

$$\int d\alpha(\dots) \frac{\alpha_{ct}^2 - \frac{\mu^2}{(D-4)}}{\rho_1 \dots \rho_N} = 0.$$

Thus if we transform accordingly all monomials in the tensor basis that contain a square of a common-transverse variable, we can move these functions to our set of surface terms, S_Γ .

Similarly, considering the case of $(\alpha_{ct})^4$,

$$\begin{aligned} \int d\alpha(\dots) \frac{\alpha_{ct}^4}{\rho_1 \dots \rho_N} &= n_\mu n_\nu n_\sigma n_\gamma \int d\alpha(\dots) \frac{\ell^\mu \ell^\nu \ell^\sigma \ell^\gamma}{\rho_1 \dots \rho_N}, \\ \int d\alpha(\dots) \frac{\ell^\mu \ell^\nu \ell^\sigma \ell^\gamma}{\rho_1 \dots \rho_N} &= C g^{(\mu\nu} g^{\sigma\gamma)} + D q^{(\mu} q^\nu g^{\sigma\gamma)} + E q^\mu q^\nu q^\sigma q^\gamma, \end{aligned}$$

where the parenthesis around the tensor indices mean that we symmetrize over all of those indices. From this, we continue the derivation in an analogous manner:

$$\begin{aligned} \begin{cases} n_\mu n_\nu n_\sigma n_\gamma \int d\alpha(\dots) \frac{\ell^\mu \ell^\nu \ell^\sigma \ell^\gamma}{\rho_1 \dots \rho_N} = \int d\alpha(\dots) \frac{\alpha_{ct}^4}{\rho_1 \dots \rho_N} = C, \\ g_{\mu\nu}^{[D-4]} g_{\sigma\gamma}^{[D-4]} \int d\alpha(\dots) \frac{\ell^\mu \ell^\nu \ell^\sigma \ell^\gamma}{\rho_1 \dots \rho_N} = \int d\alpha(\dots) \frac{\mu^4}{\rho_1 \dots \rho_N} = [(D-4)^2 + 2(D-4)] C = (D-4)(D-2)C. \end{cases} \\ \Rightarrow \int d\alpha(\dots) \frac{\alpha_{ct}^4 - \frac{\mu^4}{(D-4)(D-2)}}{\rho_1 \dots \rho_N} = 0. \end{aligned}$$

With these two transformations we can then reorganize the tensor basis functions into a new integrand basis, which we call the *scattering-plane tensor basis*, which include all monomials with only ISP variables and all surface terms constructed from the monomials with common transverse variables.

5.5 Master-Surface Basis

The scattering-plane tensor basis introduced in the previous subsection achieves part of our goal to parametrize integrands in terms of master and surface terms (as in (5.16)). But in general it still leave a lot of integrals (of ISP monomials) which are reducible according to IBP relations (see section 3.3.1). That is, with the scattering-plane tensor basis we are left with monomials, $(\alpha_t^{l_j})^{\bar{a}}$ which we will need to integrate. We use IBP relations to reduce as many of them as needed to master integrals.

Suppose we have an IBP relation,

$$I_i = \sum_j c_{ij} I'_j, \quad (5.18)$$

where I'_j are the master integrals. This implies that

$$I_i - \sum_j c_{ij} I'_j = 0. \quad (5.19)$$

Using this property, we can relate the numerator of these integrands, m_I corresponding to I and $m_{I'}$ corresponding to I' , such that

$$\int \left(\prod_l d^D \ell_l \right) \left(m_{I,i} - \sum_j c_{ij} m_{I'_j} \right) = 0. \quad (5.20)$$

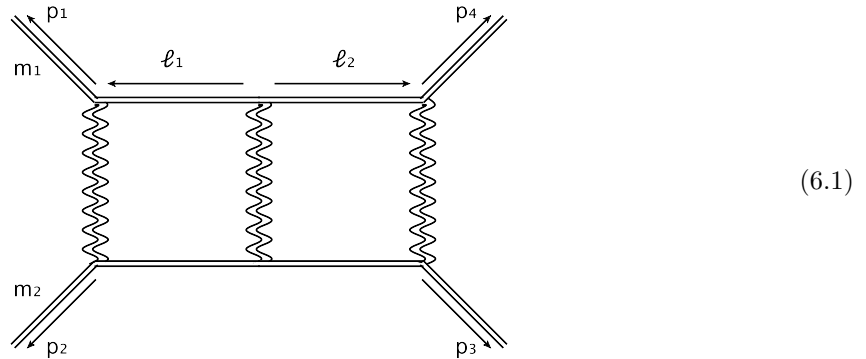
If we have a way to obtain the minimal set of master integrals, we can reduce our scattering-tensor basis to a basis of functions that only integrate to zero or to master integrals. We define this basis as the *master-surface basis*.

FIRE

To obtain the minimal set of master integrals we make use of computer program FIRE [17]. FIRE implements algorithms for reducing generic families of Feynman integrals to a set of master integrals. The most important algorithm which it implements is called the Laporta algorithm [14], to which we refer for more details. Using FIRE we can find the minimal number of master integrals and then specify our choice of master integrals. This allows us to transform the scattering-tensor basis to the master-surface basis.

6 Numerical Unitarity Method Applied to Double-Box

We employ then the numerical unitarity method introduced in section 5 for computing the key diagram we study in this document. The following diagram specify the conventions we use for loop-momenta routing, external momenta assignments and particle masses in the double-box:



The generic Feynman Integral for the double box is thus given by,

$$I(p_1, p_2, p_3, p_4; m_1^2, m_2^2; D) = \int e^{2\gamma\epsilon} \frac{d^D \ell_1}{i\pi^{D/2}} \frac{d^D \ell_2}{i\pi^{D/2}} \frac{\mathcal{N}(\{\ell_i \cdot \ell_j, \ell_m \cdot p_k\}; D)}{\rho_1 \rho_2 \rho_3 \rho_4 \rho_5 \rho_6 \rho_7}, \quad (6.2)$$

where $\mathcal{N}(\{\ell_i \cdot \ell_j, \ell_m \cdot p_k\}; D)$ is a general numerator for the double box and the propagators are given by,

$$\begin{aligned} \rho_1 &= (m_1^2 - l_1^2) , & \rho_2 &= -(l_1 - p_1)^2 , & \rho_3 &= (m_2^2 - (l_1 - p_1 - p_2)^2) , & \rho_4 &= -(l_1 + l_2)^2 , \\ \rho_5 &= (m_1^2 - l_2^2) , & \rho_6 &= -(l_2 - p_4)^2 , & \rho_7 &= (m_2^2 - (l_1 + p_1 + p_2)^2) . \end{aligned} \quad (6.3)$$

We complete the propagator structure of the double-box by introducing the following inverse propagators (see section 3.2.5),

$$\{(\ell_1 + p_4)^2, (\ell_2 + p_1)^2\} , \quad (6.4)$$

corresponding to the ISPs, $\ell_1 \cdot p_4$ and $\ell_2 \cdot p_1$. With our complete family for the double box, we can define the relevant variables for our adaptive loop-momentum parametrization as follows:

$$\alpha_1 = \ell_1 \cdot p_4 , \quad \alpha_{1,ct} = \ell_1 \cdot n_{ct} , \quad \alpha_2 = \ell_2 \cdot p_1 , \quad \alpha_{2,ct} = \ell_2 \cdot n_{ct} . \quad (6.5)$$

We also define the two functions *mu11* and *mu22* that we use in the following sections:

$$\mu_{11} = g_{\mu\nu}^{[D-4]} \ell_1^\mu \ell_1^\nu , \quad \mu_{22} = g_{\mu\nu}^{[D-4]} \ell_2^\mu \ell_2^\nu . \quad (6.6)$$

Using these definitions we first construct the double-box tensor basis. For our numerical study, we use the following variable substitutions for our numerical study:

$$d \rightarrow d , \quad s \rightarrow \frac{1}{5} , \quad t \rightarrow \frac{2}{3} , \quad m_1^2 \rightarrow \frac{11}{5} , \quad m_2^2 \rightarrow \frac{3}{17} , \quad (6.7)$$

Where s and t are the Mandelstam variables defined as,

$$s = (p_1 + p_2)^2 \quad t = (p_1 + p_4)^2 . \quad (6.8)$$

For the finite field we work in for our numerical unitary method we use prime number,

$$p = 2147483629 . \quad (6.9)$$

Working in finite number fields resembles closely the work on the rational numbers. The rational numbers form a non-algebraically closed field, like the real numbers. When doing calculations in these types of number fields within quantum field theories, it is necessary (for example to obtain manifestly real representations of the Clifford Algebra) to work with an alternating metric signature $g'_{[D]} = (+1, -1, +1, -1, \dots)$. See Ref. [4] for more details.

With all of this information, we can now form the tensor basis, then the scattering-tensor basis, and finally, employing FIRE, the master-surface basis for the double box. In the following section we describe our results for this procedure. Once we have these bases, we will use the cut-equation (see section 5.1) to find the needed master integral coefficients of our double-box.

6.1 Double-Box Tensor Basis

The integrand bases we will construct will cover generic integrands in field theory with renormalizable power counting. This means that the total power of the loop momentum in the numerator only goes to order 6 in the double-box. That is, in the tensor basis monomials will have a maximum degree of 6. We observe that this power counting is enough to describe the integrands we consider, even though the gravity theories employed in principle are non renormalizable. If they were not enough, we would simply increase the power counting to match the naively expected one.

Using the restrictions in power counting, we construct a Mathematica program to provide all the monomials present in the tensor basis. We find 160 monomials, that is, the dimension of the function space to fit generic integrands in renormalizable theories is 160. We summarize the results in table 1 below. The complete tensor basis is given in Appendix C.

Power	Monomials	Number
0	1	1
1	$\alpha_1, \alpha_{1,ct}, \alpha_2, \alpha_{2,ct}$	4
2	$\alpha_1^2, \alpha_1 \alpha_{1,ct}, \alpha_1 \alpha_2, \alpha_1 \alpha_{2,ct}, \alpha_{1,ct}^2, \dots$	10
3	$\alpha_1^3, \alpha_1^2 \alpha_{1,ct}, \alpha_1^2 \alpha_2, \alpha_1^2 \alpha_{2,ct}, \alpha_1 \alpha_{1,ct}^2, \dots$	20
4	$\alpha_1^4, \alpha_1^3 \alpha_{1,ct}, \alpha_1^3 \alpha_2, \alpha_1^3 \alpha_{2,ct}, \alpha_1^2 \alpha_{1,ct}^2, \dots$	35
5	$\alpha_1^4 \alpha_2, \alpha_1^4 \alpha_{2,ct}, \alpha_1^3 \alpha_2 \alpha_{1,ct}, \alpha_1^3 \alpha_{1,ct} \alpha_{2,ct}, \alpha_1^3 \alpha_2^2, \dots$	44
6	$\alpha_1^4 \alpha_2^2, \alpha_1^4 \alpha_2 \alpha_{2,ct}, \alpha_1^4 \alpha_{2,ct}^2, \alpha_1^3 \alpha_2^2 \alpha_{1,ct}, \alpha_1^3 \alpha_2 \alpha_{1,ct} \alpha_{2,ct}, \dots$	46
Total		160

Table 1: Summary of monomials which form the tensor basis for the double-box. Each row shows the monomials corresponding to a given power counting.

6.2 Double-Box Scattering-Plane Tensor Basis

Building from the tensor basis, and making the appropriate transformations as described in section 5.4, we arrive at a basis with 138 surface terms and 22 monomials in the ISP variables. The monomials in the ISP variables are shown in table 2, and the surface terms are shown in table 3. For the complete scattering-plane tensor basis see Appendix D.

Power	Monomials $\in M_\Gamma$	Number
0	1	1
1	α_1, α_2	2
2	$\alpha_1^2, \alpha_1 \alpha_2, \alpha_2^2$	3
3	$\alpha_1^3, \alpha_1^2 \alpha_2, \alpha_1 \alpha_2^2, \alpha_2^3$	4
4	$\alpha_1^4, \alpha_1^3 \alpha_2, \alpha_1^2 \alpha_2^2, \alpha_1 \alpha_2^3, \alpha_2^4$	5
5	$\alpha_1^4 \alpha_2, \alpha_1^3 \alpha_2^2, \alpha_1^2 \alpha_2^3, \alpha_1 \alpha_2^4$	4
6	$\alpha_1^4 \alpha_2^2, \alpha_1^3 \alpha_2^3, \alpha_1^2 \alpha_2^4$	3
Total		22

Table 2: Summary of monomials on the ISP variables for the scattering-plane tensor basis for the double-box. Each row shows the monomials corresponding to a given power counting.

Power	Monomials $\in S_\Gamma$	Number
0	\emptyset	0
1	$\alpha_{1,ct}, \alpha_{2,ct}$	2
2	$\alpha_{1,ct}^2 - \frac{\mu_{11}}{D-4}, \alpha_{2,ct}^2 - \frac{\mu_{22}}{D-4}, \alpha_1 \alpha_{1,ct}, \alpha_1 \alpha_{2,ct}, \alpha_2 \alpha_{1,ct}, \alpha_2 \alpha_{2,ct}$	7
3	$\alpha_1 \left(\alpha_{1,ct}^2 - \frac{\mu_{11}}{D-4} \right), \alpha_1 \left(\alpha_{2,ct}^2 - \frac{\mu_{22}}{D-4} \right), \dots, \alpha_1^2 \alpha_{1,ct}, \alpha_1^2 \alpha_{2,ct}, \alpha_1 \alpha_2 \alpha_{1,ct}, \dots$	16
4	$\alpha_1^2 \left(\alpha_{1,ct}^2 - \frac{\mu_{11}}{D-4} \right), \dots, \alpha_{1,ct}^4 - \frac{\mu_{11}^2}{(D-4)(D-2)}, \dots, \alpha_1^3 \alpha_{1,ct}, \alpha_1^3 \alpha_{2,ct}, \alpha_1^2 \alpha_2 \alpha_{1,ct}, \dots$	30
5	$\alpha_1^3 \left(\alpha_{2,ct}^2 - \frac{\mu_{22}}{D-4} \right), \alpha_1^2 \alpha_2 \left(\alpha_{1,ct}^2 - \frac{\mu_{11}}{D-4} \right), \dots, \alpha_1^4 \alpha_{2,ct}, \alpha_1^3 \alpha_2 \alpha_{1,ct}, \dots$	40
6	$\alpha_1^4 \left(\alpha_{2,ct}^2 - \frac{\mu_{22}}{D-4} \right), \alpha_1^3 \alpha_2 \left(\alpha_{2,ct}^2 - \frac{\mu_{22}}{D-4} \right), \dots, \alpha_1^4 \alpha_2 \alpha_{2,ct}, \alpha_1^3 \alpha_2^2 \alpha_{1,ct}, \dots$	43
Total		138

Table 3: Summary of surface terms in the scattering-plane tensor basis for the double-box. Each row shows the functions corresponding to a given power counting. Notice that the row with zero power counting has no functions.

6.3 IBP Identities for Double-Box

Using FIRE, we are able to reduce all the ISP monomials in the scattering-plane tensor basis, those shown in table 2. When we do this procedure, we see that all these monomials can be reduced on-shell (that is, setting all inverse propagators of the double-box to zero) to only two masters. FIRE allows us to make a choice of masters. We chose integrals with integrands corresponding to scattering-plane monomials with the lowest power counting. That is, we chose the scalar master integrals (power counting zero), and then we make an arbitrary choice between α_1 and α_2 (power counting one). Specifically, the master integrand terms we choose are:

$$\{1, \alpha_1\}, \quad (6.10)$$

which correspond to the set M_Γ defined in equation (5.16).

A feature worth highlighting is that when we put the loop momentum on-shell, monomials in the scattering tensor basis which are connected by an exchange of α_1 and α_2 share the same IBP relation. An example of this fact is

$$\begin{aligned} \alpha_1^2 \alpha_2 &\xrightarrow{\text{IBP}} \frac{4601\alpha_1(125383D - 418714)}{1002252(D-3)} + \frac{21169201(3d-10)}{501126(D-3)}, \\ \alpha_1 \alpha_2^2 &\xrightarrow{\text{IBP}} \frac{4601\alpha_1(125383D - 418714)}{1002252(D-3)} + \frac{21169201(3d-10)}{501126(D-3)}. \end{aligned}$$

This is due to the left-right symmetry of the double-box integral, which effectively exchanges α_1 and α_2 . For the complete list of IBP relations we generated from FIRE see Appendix E.

6.4 Double-Box Master-Surface Basis

Using the IBP relations from the previous subsection, we can construct the double-box master-surface basis. To highlight a specific example of this procedure with the double box using our choice of masters,

$$\begin{aligned} \alpha_1 \alpha_2 &\xrightarrow{\text{IBP}} \frac{4601}{867} + \frac{13803}{578} \alpha_1, \\ \Rightarrow \int d\alpha(\dots) \frac{\alpha_1 \alpha_2 - \frac{4601}{867} - \frac{13803}{578} \alpha_1}{\rho_1 \dots \rho_N} &= 0, \end{aligned}$$

Where this is under the assumption that the integral is done on-shell.³ We perform this same procedure for all the scattering-plane monomials, except for our choice of masters. The masters are already listed in equation (6.10) and the surface terms that are shared with the scattering-plane tensor basis are summarized in table 3.

The surface terms in the master-surface basis coming from the IBP relations are summarized in table 4, with only a few of the newly created terms which are not shared with the scattering plane tensor basis listed. For the complete scattering plane tensor basis, see Appendix F.

Power	Surface Terms from ISPs	Number
0	\emptyset	0
1	$\alpha_2 - \alpha_1$	1
2	$\alpha_1^2 - \frac{\alpha_1(41409D-166792)}{1734(D-3)} - \frac{4601(D-4)}{867(D-3)}, \alpha_1\alpha_2 - \frac{13803\alpha_1}{578} - \frac{4601}{867}, \dots$	3
3	$\alpha_1^3 - \frac{\alpha_1(1730661549D^2-12797893146D+23503660472)}{3006756(D-3)(D-2)} - \frac{4601(D-4)(41409D-140342)}{1503378(D-3)(D-2)}, \dots$	4
4	$\alpha_1^3\alpha_2 - \frac{4601\alpha_1(5239853451D^2-31568107186D+47007320944)}{1737904968(D-3)(D-2)} - \frac{21169201(125383D^2-754610D+1122736)}{868952484(D-3)(D-2)}, \dots$	5
5	$\alpha_1^3\alpha_2^2 - \frac{21169201\alpha_1(15864503101D^2-95188354942D+141021962832)}{1004509071504(D-3)^2} + \frac{97399493801(3D-8)(126539D-421026)}{502254535752(D-3)^2}, \dots$	4
6	$\alpha_1^3\alpha_2^3 - \frac{97399493801\alpha_1(3D-8)(5336927395D^2-24840945214D+23503660472)}{193535414443104(D-3)^2(D-2)} - \frac{97399493801(15864503101D^3-116049358466D^2+266387477208D-185965500096)}{870909364993968(D-3)^2(D-2)}, \dots$	3
Total		20

Table 4: Summary of surface terms from ISPs in the master-surface integrand basis of the double-box. The number in each row counts the monomials corresponding to a given power counting which were transformed into surface terms through IBP relations.

6.5 Cut Equation for Double-Box

Using Caravel we can now determine the coefficients for our amplitudes in each basis. Using the physical parameters defined in equation 6.5, we use caravel to study the case of two scalar black holes, which we label “ssSS”, and one scalar and one vector black hole, labelled “ssVV”. The scalar black holes correspond to non-spinning black holes while the vector black holes correspond to spinning black holes.

6.5.1 ssSS Scattering Process

Using the cut equation and the product of trees calculated by Caravel we determine that there is only one non-zero coefficient corresponding to the monomial 1. This coefficient takes the form,

$$c_{\Gamma,1} = 1347859965. \quad (6.11)$$

This result is consistent in each basis. This simplicity is expected from earlier calculations of the ssSS process.

³This is only to simplify the discussion, and because this is what we need for the scope of this work.

6.5.2 ssVV Scattering Process

Again, using the cut equation and the product of trees calculated for the ssVV case, we determine that there are 29 non-zero coefficients. In the tensor basis, there are 13 non-zero coefficients which correspond to monomials without odd powers of common transverse variables. Meaning that there are 13 coefficients that will survive when we integrate the integrand. In the scattering-plane tensor basis, there are 9 non-zero coefficients which correspond to master terms. The two coefficients of most interest are the terms corresponding to our choice master integral in the master-surface basis. We report these coefficients for each basis bellow, with the other 27 being found in ancillary files detailed in section 6.7.

$$\begin{aligned}
& c_{\Gamma,1} = 872787083, \\
\text{Tensor Basis:} \quad & c_{\Gamma,\alpha_1} = 114476361, \\
& \dots
\end{aligned} \tag{6.12}$$

$$\begin{aligned}
& c_{\Gamma,1} = \frac{872787083D + 535800955}{D + 1877880711}, \\
\text{Scattering-Plane Tensor Basis:} \quad & c_{\Gamma,\alpha_1} = \frac{114476361D + 228459914}{D + 1877880711}, \\
& \dots
\end{aligned} \tag{6.13}$$

$$\begin{aligned}
& c_{\Gamma,1} = \frac{542956566D^3 + 730446438D^2 + 874308839D + 977509702}{D^3 + 1877880705D^2 + 1617617517D + 1868540996}, \\
\text{Master-Surface Basis:} \quad & c_{\Gamma,\alpha_1} = \frac{292690379D^3 + 1591077384D^2 + 1858212605D + 524076769}{D^3 + 1877880705D^2 + 1617617517D + 1868540996}.
\end{aligned} \tag{6.14}$$

We can now use these coefficients and each basis to solve for the numeric expression of the integrand at different points in phase space.

6.6 Validation

To check these results, we can sample over different points in phase space than that used to calculate the coefficients and verify that the amplitude we calculate using each basis agrees with the amplitude calculated by Caravel at these new points in on-shell phase space. This is called the $N = N$ validation check. This check is trivial for the ssSS case, as the amplitude is always the same regardless of our choice of point in phase space. For the ssVV case, however, we have a more complicated coefficient structure, therefore giving us a non-trivial check of our calculation.

Performing the $N = N$ validation check we find that the amplitude we calculate using our coefficients for each basis agree with the independent calculation of the amplitude by Caravel across three separate on-shell phase-space points. We give all details for this validation procedure in the ancillary files detailed in section 6.7. This confirms that our results do provide the parametrization of the double box we set out to find.

6.7 Ancillary files

To see all the files used in our study of the two-loop double box with massive particles, visit the GitLab for this project: <https://gitlab.com/RobertLaughlin/tensor-integrals.git>

This GitLab contains the files used to create the parametrization, solve for the coefficients, and validate our parametrization. Details on the Files are included in the README file of the GitLab repository.

7 Conclusion and Outlook

We have successfully parametrized the two-loop double box with massive particles using adaptive loop momentum parametrization and IBP relations. This parametrization can be used in calculations of gravitational potentials in binary black hole systems to third order in Newton's constant $\mathcal{O}(G^3)$. This parametrization can simplify related computations. Further, this parametrization can now be used to study other two-loop Feynman diagrams which are related to the two-loop double-box studied in this work.

We got these results by completing the propagator structure for the two-loop double-box to obtain our ISPs and allow us to take cuts of the two-loop double-box. Then, using adaptive loop momentum parametrization on the two-loop double-box Feynman integral, we represented the numerator of the scattering amplitude integrand in the tensor basis. We further reduce the tensor basis by transforming monomials containing common-transvers variables into surface terms, forming the scattering plane tensor basis. Finally, with the help of FIRE, we used our IBP relations to form the master-surface basis. We have used this parametrization to calculate the integrands of two scattering process of black hole interactions (ssSS and ssVV) using the cut-equation and product of trees calculated by `Caravel`.

There are many future directions to take our study of the parametrization of the two-loop double-box. With our results we could reconstruct the analytic form of the master-integral coefficients with the numerical samples that we produce. Additionally, there was a clear symmetry between the α_1 and α_2 terms used in the construction of our parametrization. The integrand parametrization we built gives us the flexibility to redefine master integrals easily. In the future, we might choose the more symmetric form, $\alpha_1 + \alpha_2$. Then, we can use FIRE to determine the integration by parts relations between the monomials with this new choice of master integrals. This may affect the number of non-zero coefficients we have in the master-surface basis. Redefinitions of functions for the subspace of surface terms might reduce the number of non-zero coefficients. In the future we could explore finding functions for the subspace of surface terms which minimizes the number of non-zero coefficients in our parametrization for the ssVV case.

Our parametrization has the flexibility to study more scattering processes. In the future, we might apply this to the vector-vector (vvVV) scattering process, corresponding to two spinning black holes, which can give conservative potential terms which look like $\vec{S}_1 \cdot \vec{S}_2$. Once we have obtained this parametrization we could search for the analytic expression of the coefficients in the parametrization of the vvVV scattering process case as well. With all these different directions to take our study of the parametrization, we see that our work opens many doors for further research.

Appendices

A Relativity

This paper assumes that the reader has a working understanding of special relativity. This Appendix quotes the main results from special relativity which are used throughout this paper. For a more complete understanding of special relativity see *Theory of Special Relativity* by Nadia L. Zakamska [19].

Special Relativity

In physics, we are primarily interested in tracking the position and movement of objects. Typically, these are measured by the spatial coordinates and momentum of the object, respectively, relative to some reference frame. Reference frames are defined by a coordinate system to measure positions and a clock to measure changes in positions [19]. An inertial reference frame is one in which time and space translational and rotational symmetries are respected and in which free particles moving at a constant speed keep their velocity.

In classical mechanics, objects are characterized by spatial coordinates and linear momentum with time as a parameter. This characterization of position and momentum is expressed in the following forms, respectively:

$$\vec{x}(t) = (x(t), y(t), z(t)) ; \quad (\text{A.1})$$

$$\vec{p}(t) = (p_x(t), p_y(t), p_z(t)) ; \quad (\text{A.2})$$

In special relativity, we find we need to think of time as being relative to the reference frame. This result came as a consequence of a maximum signal speed (that experimentally is observed to be the speed of light in a vacuum) which is the same regardless of reference frame and of the principle that fundamental laws of physics remain the same regardless of inertial reference frame. As time is now relative, we must go from our spatial 3-vectors and momentum 3-vectors to spatial 4-vectors and momentum 4-vector.

$$x = (ct, x, y, z) ; \quad (\text{A.3})$$

$$p = \left(\frac{E}{c}, p_x, p_y, p_z\right) ; \quad (\text{A.4})$$

In special relativity, we must define a metric tensor which allows us to express our equations in covariant form, i.e. the equation is true in every reference frame. Here we use the (+ - - -) metric signature

$$\eta^{\mu\nu} = \begin{bmatrix} 1 & 0 & 0 & 0 \\ 0 & -1 & 0 & 0 \\ 0 & 0 & -1 & 0 \\ 0 & 0 & 0 & -1 \end{bmatrix} , \quad (\text{A.5})$$

and

$$\eta_{\mu\nu} = \begin{bmatrix} 1 & 0 & 0 & 0 \\ 0 & -1 & 0 & 0 \\ 0 & 0 & -1 & 0 \\ 0 & 0 & 0 & -1 \end{bmatrix} . \quad (\text{A.6})$$

to translate between two inertial reference frames we take a Lorentz transformation between the two frames. For a boost in the x-direction, this Lorentz transform takes the form

$$\Lambda^\mu{}_\nu = \begin{bmatrix} \cosh(\eta) & -\sinh(\eta) & 0 & 0 \\ -\sinh(\eta) & \cosh(\eta) & 0 & 0 \\ 0 & 0 & 1 & 0 \\ 0 & 0 & 0 & 1 \end{bmatrix} , \quad (\text{A.7})$$

where $\cosh(\eta) = \frac{1}{\sqrt{1-\frac{U^2}{c^2}}}$ and $\sinh(\eta) = \frac{1}{\sqrt{1-\frac{U^2}{c^2}}} \frac{U}{c}$ with U being the velocity of one inertial frame with respect to the other.

In order to maintain covariant equations, our operators must also be four vectors and four tensors. One operator that we make use of frequently is the partial derivative operator ∂^μ which takes the form

$$\partial_\mu = \left(\frac{1}{c} \frac{\partial}{\partial t}, \frac{\partial}{\partial x}, \frac{\partial}{\partial y}, \frac{\partial}{\partial z} \right). \quad (\text{A.8})$$

The final important result we will provide is the relativistic dispersion relation. This is a consequence of the invariance of 4-scalars. Therefore,

$$p_\mu p^\mu = p^2 = \text{constant}. \quad (\text{A.9})$$

In the frame of the particle $p = \left(\frac{E}{c}, \vec{0} \right)$, where $\frac{E}{c} \equiv \frac{mc}{\sqrt{1-\left(\frac{v}{c}\right)^2}}$. $p^2 = (mc)^2$, therefore by the invariance of 4-scalars,

$$p^2 = \left(\frac{E}{c} \right)^2 - \vec{p} \cdot \vec{p} = (mc)^2. \quad (\text{A.10})$$

or in the more standard form

$$E^2 = c^2 \vec{p} \cdot \vec{p} + (mc^2)^2. \quad (\text{A.11})$$

This equation, known as the relativistic dispersion relation is an important result used for the development of QFT.

Keep in mind that throughout this paper we used natural units $\hbar = c = 1$. In this Appendix, we have shown c explicitly to make the notation more familiar.

B Alternate approach to Master-Surface Parametrization

Before the use of adaptive parametrization was used for master-surface decomposition, an a different method was used. Although we did not use this method for our study of the double box, we include the general theory to provide a historical perspective of the methods used.

If we have a generic Feynman integral numerator $\mathcal{N} = \mathcal{N}(\{k_i \cdot k_j; k_i \cdot p_m\}; D)$ which is a polynomial in $k_i \cdot k_j$ and $k_i \cdot p_m$, we construct an ansatz

$$\mathcal{N}_\Gamma = \sum_{i \in Q_\Gamma} c_{\Gamma,i} m_{\Gamma,i}(\{k_i \cdot k_j; k_i \cdot p_m\}; D) , \quad (\text{B.1})$$

where Γ is a propagator structure $\{\rho_1, \dots, \rho_p\}$ with $\rho_k = m_k^2 - k_k^2 - i\epsilon$, $c_{\Gamma,i}$ is a coefficient function of $p_i \cdot p_j$ and D , and $\{m_{\Gamma,i}\}$ is a set of functions.

We say that $\{m_{\Gamma,i}\}$ is a master/surface basis if $Q_\Gamma = M_\Gamma \cup S_\Gamma$ such that

$$\int \left(\prod_{i=1}^L e^{\gamma\epsilon} \frac{d^D k}{i\pi^{D/2}} \right) \frac{m_{\Gamma,i}(\{k_i \cdot k_j; k_i \cdot p_m\}; D)}{\rho_1 \dots \rho_p} = I_{\Gamma,i} \quad i \in M_\Gamma , \quad (\text{B.2})$$

where $I_{\Gamma,i}$ is a master integral, and

$$\int \left(\prod_{i=1}^L e^{\gamma\epsilon} \frac{d^D k}{i\pi^{D/2}} \right) \frac{m_{\Gamma,i}(\{k_i \cdot k_j; k_i \cdot p_m\}; D)}{\rho_1 \dots \rho_p} = 0 \quad i \in S_\Gamma . \quad (\text{B.3})$$

Linear algebra allows us to fix our $c_{\Gamma,i}$ as constants. So now we need a method to generate these $\{m_i\}$. Suppose we have an IBP relation, $I_1 = c_{11}I'_1 + c_{12}I'_2$.

$$\Rightarrow I_1 - c_{11}I'_1 - c_{12}I'_2 = 0 .$$

We could then generate a surface term of our Feynman integrals from I_1, I'_1 , and I'_2 . The other technique we will use to generate surface terms will be by using equation (3.36),

$$\int \frac{d^D k_j}{(i\pi^{D/2})} \frac{\partial}{\partial k_j^\mu} \left(\frac{t_r(k_l) u_j^\mu}{\rho_1 \dots \rho_p} \right) = 0 , \quad (\text{B.4})$$

where $\rho_k = m_k^2 - k_k^2 - i\epsilon$ as before, u_j^μ is a unitary compatible IBP-generating vector, and $t_r(k_l)$ is some function of the loop momentum.

$$\begin{aligned} & \int \frac{d^D k_j}{(i\pi^{D/2})} \frac{\partial}{\partial k_j^\mu} \left(\frac{t_r(k_l) u_j^\mu}{\rho_1 \dots \rho_p} \right) = 0 , \\ & \int \frac{d^D k_j}{(i\pi^{D/2})} \left(\frac{\partial t_r(k_l)}{\partial k_j^\mu} \frac{u_j^\mu}{\rho_1 \dots \rho_p} + t_r(k_l) \left(\frac{1}{\rho_1 \dots \rho_p} \frac{\partial u_j^\mu}{\partial k_j^\mu} - \frac{u_j^\mu}{\rho_1 \dots \rho_p} \sum_{k \in p_\Gamma} \frac{\partial \rho_k}{\partial k_j^\mu} \frac{1}{\rho_k} \right) \right) = 0 . \end{aligned}$$

we then apply the following condition,

$$u_j^\mu \frac{\partial}{\partial k_j^\mu} \rho_k = f_k \rho . \quad (\text{B.5})$$

This condition is know as the Syzygy equation [12]. When applied we yield,

$$\int \frac{d^D k_j}{(i\pi^{D/2})} \frac{1}{\rho_1 \dots \rho_p} \left(u_j^\mu \frac{\partial t_r(k_l)}{\partial k_j^\mu} + t_r(k_l) \left(\frac{\partial u_j^\mu}{\partial k_j^\mu} - \sum_{k \in p_\Gamma} f_k \right) \right) = 0 . \quad (\text{B.6})$$

Comparing equation (B.6) to (B.3) we see that

$$m_\Gamma = u_j^\mu \frac{\partial t_r(k_l)}{\partial k_j^\mu} + t_r(k_l) \left(\frac{\partial u_j^\mu}{\partial k_j^\mu} - \sum_{k \in p_\Gamma} f_k \right) . \quad (\text{B.7})$$

This equation provides us a way to industrially produce surface terms [2]. Using this equation we will be able to decompose a chosen family of Feynman integrals into surface and master integrals.

C Double-Box Tensor Basis

The entire tensor basis for the double box is expressed below.

[illegible]

D Double-Box Scattering Tensor Basis

The entire scattering tensor basis for the double box is expressed below.

$$\begin{aligned}
& \{ \{ 1, \alpha_1, \alpha_2, \alpha_1^2, \alpha_1\alpha_2, \alpha_2^2, \alpha_1^3, \alpha_1^2\alpha_2, \alpha_1\alpha_2^2, \alpha_2^3, \alpha_1^4, \alpha_1^3\alpha_2, \alpha_1^2\alpha_2^2, \alpha_1\alpha_2^3, \alpha_2^4, \alpha_1^4\alpha_2, \alpha_1^3\alpha_2^2, \alpha_1^2\alpha_2^3, \\
& \alpha_1\alpha_2^4, \alpha_1^4\alpha_2^2, \alpha_1^3\alpha_2^3, \alpha_1^2\alpha_2^4 \}, \{ \alpha_{1,ct}^2 - \mu_{11}/(-4+D), \alpha_{2,ct}^2 - \mu_{22}/(-4+D), \\
& \alpha_1(\alpha_{1,ct}^2 - \mu_{11}/(-4+D)), \alpha_1(\alpha_{2,ct}^2 - \mu_{22}/(-4+D)), \alpha_2(\alpha_{1,ct}^2 - \mu_{11}/(-4+D)), \\
& \alpha_2(\alpha_{2,ct}^2 - \mu_{22}/(-4+D)), \alpha_1^2(\alpha_{1,ct}^2 - \mu_{11}/(-4+D)), \alpha_1^2(\alpha_{2,ct}^2 - \mu_{22}/(-4+D)), \\
& \alpha_1\alpha_2(\alpha_{1,ct}^2 - \mu_{11}/(-4+D)), \alpha_1\alpha_2(\alpha_{2,ct}^2 - \mu_{22}/(-4+D)), \alpha_{1,ct}^4 - \mu_{11}^2/((-4+D)(-2+D)), \\
& \alpha_2^2(\alpha_{1,ct}^2 - \mu_{11}/(-4+D)), (\alpha_{1,ct}^2 - \mu_{11}/(-4+D))(\alpha_{2,ct}^2 - \mu_{22}/(-4+D)), \alpha_2^2(\alpha_{2,ct}^2 - \mu_{22}/(-4+D)), \\
& \alpha_{2,ct}^4 - \mu_{22}^2/((-4+D)(-2+D)), \alpha_1^3(\alpha_{2,ct}^2 - \mu_{22}/(-4+D)), \alpha_1^2\alpha_2(\alpha_{1,ct}^2 - \mu_{11}/(-4+D)), \\
& \alpha_1^2\alpha_2(\alpha_{2,ct}^2 - \mu_{22}/(-4+D)), \alpha_1\alpha_2^2(\alpha_{1,ct}^2 - \mu_{11}/(-4+D)), \\
& \alpha_1(\alpha_{1,ct}^2 - \mu_{11}/(-4+D))(\alpha_{2,ct}^2 - \mu_{22}/(-4+D)), \alpha_1\alpha_2^2(\alpha_{2,ct}^2 - \mu_{22}/(-4+D)), \\
& \alpha_1(\alpha_{2,ct}^4 - \mu_{22}^2/((-4+D)(-2+D))), \alpha_2(\alpha_{1,ct}^4 - \mu_{11}^2/((-4+D)(-2+D))), \\
& \alpha_2^3(\alpha_{1,ct}^2 - \mu_{11}/(-4+D)), \alpha_2(\alpha_{1,ct}^2 - \mu_{11}/(-4+D))(\alpha_{2,ct}^2 - \mu_{22}/(-4+D)), \\
& \alpha_1^4(\alpha_{2,ct}^2 - \mu_{22}/(-4+D)), \alpha_1^3\alpha_2(\alpha_{2,ct}^2 - \mu_{22}/(-4+D)), \alpha_1^2\alpha_2^2(\alpha_{1,ct}^2 - \mu_{11}/(-4+D)), \\
& \alpha_1^2(\alpha_{1,ct}^2 - \mu_{11}/(-4+D))(\alpha_{2,ct}^2 - \mu_{22}/(-4+D)), \alpha_1^2\alpha_2^2(\alpha_{2,ct}^2 - \mu_{22}/(-4+D)), \\
& \alpha_1^2(\alpha_{2,ct}^4 - \mu_{22}^2/((-4+D)(-2+D))), \alpha_1\alpha_2^3(\alpha_{1,ct}^2 - \mu_{11}/(-4+D)), \\
& \alpha_1\alpha_2(\alpha_{1,ct}^2 - \mu_{11}/(-4+D))(\alpha_{2,ct}^2 - \mu_{22}/(-4+D)), \alpha_2^2(\alpha_{1,ct}^4 - \mu_{11}^2/((-4+D)(-2+D))), \\
& (\alpha_{1,ct}^4 - \mu_{11}^2/((-4+D)(-2+D))) (\alpha_{2,ct}^2 - \mu_{22}/(-4+D)), \alpha_2^4(\alpha_{1,ct}^2 - \mu_{11}/(-4+D)), \\
& \alpha_2^2(\alpha_{1,ct}^2 - \mu_{11}/(-4+D))(\alpha_{2,ct}^2 - \mu_{22}/(-4+D)), \\
& (\alpha_{1,ct}^4 - \mu_{11}^2/(-4+D))(\alpha_{2,ct}^4 - \mu_{22}^2/((-4+D)(-2+D))), \alpha_{1,ct}, \alpha_{2,ct}, \alpha_1\alpha_{1,ct}, \alpha_1\alpha_{2,ct}, \alpha_2\alpha_{1,ct}, \\
& \alpha_{1,ct}\alpha_{2,ct}, \alpha_2\alpha_{2,ct}, \alpha_1^2\alpha_{1,ct}, \alpha_1^2\alpha_{2,ct}, \alpha_1\alpha_2\alpha_{1,ct}, \alpha_1\alpha_{1,ct}\alpha_{2,ct}, \alpha_1\alpha_2\alpha_{2,ct}, \alpha_{1,ct}^3, \alpha_{1,ct}^2\alpha_{2,ct}, \\
& \alpha_2^2\alpha_{1,ct}, \alpha_2\alpha_{1,ct}\alpha_{2,ct}, \alpha_{1,ct}\alpha_{2,ct}^2, \alpha_2^2\alpha_{2,ct}, \alpha_{2,ct}^3, \alpha_1^3\alpha_{1,ct}, \alpha_1^3\alpha_{2,ct}, \alpha_1^2\alpha_2\alpha_{1,ct}, \alpha_1^2\alpha_{1,ct}\alpha_{2,ct}, \\
& \alpha_1^2\alpha_2\alpha_{2,ct}, \alpha_1\alpha_{1,ct}^3, \alpha_1\alpha_{1,ct}^2\alpha_{2,ct}, \alpha_1\alpha_{1,ct}^2\alpha_{1,ct}, \alpha_1\alpha_2\alpha_{1,ct}\alpha_{2,ct}, \alpha_1\alpha_{1,ct}\alpha_{2,ct}^2, \alpha_1\alpha_2^2\alpha_{2,ct}, \alpha_1\alpha_{2,ct}^3, \\
& \alpha_2\alpha_{1,ct}^3, \alpha_{1,ct}^3\alpha_{2,ct}, \alpha_2\alpha_{1,ct}^2\alpha_{2,ct}, \alpha_2^3\alpha_{1,ct}, \alpha_2^2\alpha_{1,ct}\alpha_{2,ct}, \alpha_2\alpha_{1,ct}\alpha_{2,ct}^2, \alpha_{1,ct}\alpha_{2,ct}^3, \alpha_2^3\alpha_{2,ct}, \\
& \alpha_2\alpha_{2,ct}^3, \alpha_1^4\alpha_{2,ct}, \alpha_1^3\alpha_2\alpha_{1,ct}, \alpha_1^3\alpha_{1,ct}\alpha_{2,ct}, \alpha_1^3\alpha_2\alpha_{2,ct}, \alpha_1^2\alpha_{1,ct}^2\alpha_{2,ct}, \alpha_1^2\alpha_2^2\alpha_{1,ct}, \alpha_1^2\alpha_2\alpha_{1,ct}\alpha_{2,ct}, \\
& \alpha_1^2\alpha_{1,ct}\alpha_{2,ct}^2, \alpha_1^2\alpha_2^2\alpha_{2,ct}, \alpha_1^2\alpha_{2,ct}^3, \alpha_1\alpha_2\alpha_{1,ct}^3, \alpha_1\alpha_{1,ct}^3\alpha_{2,ct}, \alpha_1\alpha_2\alpha_{1,ct}^2\alpha_{2,ct}, \alpha_1\alpha_2^3\alpha_{1,ct}, \\
& \alpha_1\alpha_2^2\alpha_{1,ct}\alpha_{2,ct}, \alpha_1\alpha_2\alpha_{1,ct}\alpha_{2,ct}^2, \alpha_1\alpha_{1,ct}\alpha_{2,ct}^3, \alpha_1\alpha_2^3\alpha_{2,ct}, \alpha_1\alpha_2\alpha_{2,ct}^3, \alpha_{1,ct}^4\alpha_{2,ct}, \alpha_{2,ct}^2\alpha_{1,ct}^3, \\
& \alpha_2\alpha_{1,ct}^3\alpha_{2,ct}, \alpha_{1,ct}^3\alpha_{2,ct}^2, \alpha_2^2\alpha_{1,ct}^2\alpha_{2,ct}, \alpha_{1,ct}^2\alpha_{2,ct}^3, \alpha_2^2\alpha_{1,ct}\alpha_{2,ct}, \alpha_2^2\alpha_{1,ct}\alpha_{2,ct}^2, \\
& \alpha_2\alpha_{1,ct}\alpha_{2,ct}^3, \alpha_{1,ct}\alpha_{2,ct}^4, \alpha_1^4\alpha_2\alpha_{2,ct}, \alpha_1^3\alpha_2^2\alpha_{1,ct}, \alpha_1^3\alpha_2\alpha_{1,ct}\alpha_{2,ct}, \alpha_1^3\alpha_{1,ct}\alpha_{2,ct}^2, \alpha_1^3\alpha_2^2\alpha_{2,ct}, \alpha_1^3\alpha_2\alpha_{2,ct}^3, \\
& \alpha_1^2\alpha_2\alpha_{1,ct}^2\alpha_{2,ct}, \alpha_1^2\alpha_2^3\alpha_{1,ct}, \alpha_1^2\alpha_2^2\alpha_{1,ct}\alpha_{2,ct}, \alpha_1^2\alpha_2\alpha_{1,ct}\alpha_{2,ct}^2, \alpha_1^2\alpha_{1,ct}\alpha_{2,ct}^3, \alpha_1^2\alpha_2^3\alpha_{2,ct}, \alpha_1^2\alpha_2^2\alpha_{2,ct}, \\
& \alpha_1\alpha_2^2\alpha_{1,ct}^3, \alpha_1\alpha_2\alpha_{1,ct}^3\alpha_{2,ct}, \alpha_1\alpha_{1,ct}^3\alpha_{2,ct}^2, \alpha_1\alpha_2^2\alpha_{1,ct}\alpha_{2,ct}, \alpha_1\alpha_{1,ct}^2\alpha_{2,ct}^3, \alpha_1\alpha_{2,ct}^4\alpha_{1,ct}, \\
& \alpha_1\alpha_2^3\alpha_{1,ct}\alpha_{2,ct}, \alpha_1\alpha_2^2\alpha_{1,ct}\alpha_{2,ct}^2, \alpha_1\alpha_2\alpha_{1,ct}\alpha_{2,ct}^3, \alpha_1\alpha_{1,ct}\alpha_{2,ct}^4, \alpha_2\alpha_{1,ct}^4\alpha_{2,ct}, \alpha_{2,ct}^3\alpha_{1,ct}^3, \\
& \alpha_{2,ct}^2\alpha_{1,ct}^3\alpha_{2,ct}, \alpha_2\alpha_{1,ct}^3\alpha_{2,ct}^2, \alpha_{1,ct}^3\alpha_{2,ct}^3, \alpha_2^3\alpha_{1,ct}^2\alpha_{2,ct}, \alpha_2\alpha_{1,ct}^2\alpha_{2,ct}^3 \} \}
\end{aligned}$$

E IBP Identities for Double-Box

Using FIRE we were able to produce the IBP relations for the double box listed below. in FIRE notation, the integrand is expressed as $F[1, \{\nu_1, \nu_2, \nu_3, \nu_4, \nu_5, \nu_6, \nu_7, \nu_8, \nu_9\}]$, where each ν_i correspond to the power of ith inverse propagator in the Feynman integral. The double box has seven propagators, so ν_8 and ν_9 should be understood to correspond to the inverse propagators we introduced to complete the family for double box Feynman diagram. Therefore, we can understand ν_8 to correspond to the power of α_1 and ν_9 to correspond to the power of α_2 in our monomial. Our command *//Monomial* translates the result of the IBP relation that FIRE returns into our notation for the master integrals $\{1, \alpha_1\}$.

```

F[1, {1, 1, 1, 1, 1, 1, 1, 0, 0}] // Monomial
1
F[1, {1, 1, 1, 1, 1, 1, 1, -1, 0}] // Monomial
α1
F[1, {1, 1, 1, 1, 1, 1, 1, 0, -1}] // Monomial
α1
F[1, {1, 1, 1, 1, 1, 1, 1, -1, -1}] // Monomial
13803α1 + 4601
578 867
F[1, {1, 1, 1, 1, 1, 1, 1, 0, -2}] // Monomial
α1(41409d-166792) + 4601(D-4)
1734(D-3) 867(D-3)
F[1, {1, 1, 1, 1, 1, 1, 1, -2, 0}] // Monomial
α1(41409d-166792) + 4601(D-4)
1734(D-3) 867(D-3)
F[1, {1, 1, 1, 1, 1, 1, 1, -2, -1}] // Monomial
4601α1(125383D-418714) + 21169201(3D-10)
1002252(D-3) 501126(D-3)
F[1, {1, 1, 1, 1, 1, 1, 1, -1, -2}] // Monomial
4601α1(125383D-418714) + 21169201(3D-10)
1002252(D-3) 501126(D-3)
F[1, {1, 1, 1, 1, 1, 1, 1, -3, 0}] // Monomial
α1(1730661549D2-12797893146D+23503660472) + 4601(D-4)(41409D-140342)
3006756(D-3)(D-2) 1503378(D-3)(D-2)
F[1, {1, 1, 1, 1, 1, 1, 1, 0, -3}] // Monomial
α1(1730661549D2-12797893146D+23503660472) + 4601(D-4)(41409D-140342)
3006756(D-3)(D-2) 1503378(D-3)(D-2)
F[1, {1, 1, 1, 1, 1, 1, 1, -2, -2}] // Monomial
21169201(125383D2-751142D+1111176) + 21169201α1(3D-10)(126539D-337052)
868952484(D-3)2 579301656(D-3)2
F[1, {1, 1, 1, 1, 1, 1, 1, -3, -1}] // Monomial
4601α1(5239853451D2-31568107186D+47007320944) + 21169201(125383D2-754610D+1122736)
1737904968(D-3)(D-2) 868952484(D-3)(D-2)
F[1, {1, 1, 1, 1, 1, 1, 1, -1, -3}] // Monomial
4601α1(5239853451D2-31568107186D+47007320944) + 21169201(125383D2-754610D+1122736)
1737904968(D-3)(D-2) 868952484(D-3)(D-2)
F[1, {1, 1, 1, 1, 1, 1, 1, -4, 0}] // Monomial
4601(D-4)(576887183D2-3519829414D+5327943688) +
868952484(D-3)(D-2)(D-1)
α1(24108565728051D3-243679768825634D2+812054492791264D-892292966159008)
1737904968(D-3)(D-2)(D-1)
F[1, {1, 1, 1, 1, 1, 1, 1, 0, -4}] // Monomial
4601(D-4)(576887183D2-3519829414D+5327943688) +
868952484(D-3)(D-2)(D-1)
α1(24108565728051D3-243679768825634D2+812054492791264D-892292966159008)
1737904968(D-3)(D-2)(D-1)
...

```

$$\begin{aligned}
& F[1, \{1, 1, 1, 1, 1, 1, -1, -4\}] // \text{ Monomial} \\
& \frac{4601\alpha_1(218977736303103D^3 - 1763954877049344D^2 + 4647281343312980D - 4001733231962720)}{3013527214512(D-3)(D-2)(D-1)} + \\
& \frac{21169201(5239853451D^3 - 42176800568D^2 + 111050449684D - 95578515680)}{1506763607256(D-3)(D-2)(D-1)} \\
& F[1, \{1, 1, 1, 1, 1, 1, -4, -1\}] // \text{ Monomial} \\
& \frac{4601\alpha_1(218977736303103D^3 - 1763954877049344D^2 + 4647281343312980D - 4001733231962720)}{3013527214512(D-3)(D-2)(D-1)} + \\
& \frac{21169201(5239853451D^3 - 42176800568D^2 + 111050449684D - 95578515680)}{1506763607256(D-3)(D-2)(D-1)} \\
& F[1, \{1, 1, 1, 1, 1, 1, -2, -3\}] // \text{ Monomial} \\
& \frac{21169201\alpha_1(15864503101D^2 - 95188354942D + 141021962832)}{1004509071504(D-3)^2} + \frac{97399493801(3D-8)(126539D-421026)}{502254535752(D-3)^2} \\
& F[1, \{1, 1, 1, 1, 1, 1, -3, -2\}] // \text{ Monomial} \\
& \frac{21169201\alpha_1(15864503101D^2 - 95188354942D + 141021962832)}{1004509071504(D-3)^2} + \frac{97399493801(3D-8)(126539D-421026)}{502254535752(D-3)^2} \\
& F[1, \{1, 1, 1, 1, 1, 1, -3, -3\}] // \text{ Monomial} \\
& \frac{97399493801\alpha_1(3D-8)(5336927395D^2 - 24840945214D + 23503660472)}{193535414443104(D-3)^2(D-2)} + \\
& \frac{97399493801(15864503101D^3 - 116049358466D^2 + 266387477208D - 185965500096)}{870909364993968(D-3)^2(D-2)} \\
& F[1, \{1, 1, 1, 1, 1, 1, -4, -2\}] // \text{ Monomial} \\
& \frac{21169201\alpha_1(662990479498665D^3 - 4872230078680774D^2 + 11258936570700304D - 7949126000914176)}{1741818729987936(D-3)^2(D-1)} + \\
& \frac{97399493801(15864503101D^3 - 116488195718D^2 + 269017828048D - 189859148544)}{870909364993968(D-3)^2(D-1)} \\
& F[1, \{1, 1, 1, 1, 1, 1, -2, -4\}] // \text{ Monomial} \\
& \frac{21169201\alpha_1(662990479498665D^3 - 4872230078680774D^2 + 11258936570700304D - 7949126000914176)}{1741818729987936(D-3)^2(D-1)} + \\
& \frac{97399493801(15864503101D^3 - 116488195718D^2 + 269017828048D - 189859148544)}{870909364993968(D-3)^2(D-1)}
\end{aligned}$$

F Double-Box Master-Surface Basis

The complete master-surface basis for the double box is presented below. The master terms are presented in the first list, while the surface terms are presented in the second list.

$$\begin{aligned}
& \{1, \alpha_1\}, \\
& \{\alpha_2 - \alpha_1, \alpha_1^2 - \frac{(41409D-166792)\alpha_1}{1734(D-3)} - \frac{4601(D-4)}{867(D-3)}, \alpha_2\alpha_1 - \frac{13803\alpha_1}{578} - \frac{4601}{867}, \\
& \alpha_2^2 - \frac{4601(D-4)}{867(D-3)} - \frac{(41409D-166792)\alpha_1}{1734(D-3)}, \\
& \alpha_1^3 - \frac{(1730661549D^2-12797893146D+23503660472)\alpha_1}{3006756(D-3)(D-2)} - \frac{4601(D-4)(41409D-140342)}{1503378(D-3)(D-2)}, \\
& \alpha_2\alpha_1^2 - \frac{4601(125383D-418714)\alpha_1}{1002252(D-3)} - \frac{501126(D-3)}{501126(D-3)}, \\
& \alpha_1\alpha_2^2 - \frac{21169201(3D-10)}{501126(D-3)} - \frac{4601(125383D-418714)\alpha_1}{1002252(D-3)}, \\
& \alpha_2^3 - \frac{4601(D-4)(41409D-140342)}{1503378(D-3)(D-2)} - \frac{(1730661549D^2-12797893146D+23503660472)\alpha_1}{3006756(D-3)(D-2)}, \\
& \alpha_1^4 - \frac{(24108565728051D^3-243679768825634D^2+812054492791264D-892292966159008)\alpha_1}{1737904968(D-3)(D-2)(D-1)} - \\
& \frac{4601(D-4)(576887183D^2-3519829414D+5327943688)}{868952484(D-3)(D-2)(D-1)}, \\
& \alpha_2\alpha_1^3 - \frac{4601(5239853451D^2-31568107186D+47007320944)\alpha_1}{1737904968(D-3)(D-2)} - \frac{21169201(125383D^2-754610D+1122736)}{868952484(D-3)(D-2)}, \\
& \alpha_1^2\alpha_2^2 - \frac{21169201(3D-10)(126539D-337052)\alpha_1}{579301656(D-3)^2} - \frac{21169201(125383D^2-751142D+1111176)}{868952484(D-3)^2}, \\
& \alpha_1\alpha_2^3 - \frac{21169201(125383D^2-754610D+1122736)}{868952484(D-3)(D-2)} - \frac{4601(5239853451D^2-31568107186D+47007320944)\alpha_1}{1737904968(D-3)(D-2)}, \\
& \alpha_2^4 - \frac{4601(D-4)(576887183D^2-3519829414D+5327943688)}{868952484(D-3)(D-2)(D-1)} - \\
& \frac{(24108565728051D^3-243679768825634D^2+812054492791264D-892292966159008)\alpha_1}{1737904968(D-3)(D-2)(D-1)}, \\
& \alpha_2\alpha_1^4 - \frac{4601(218977736303103D^3-1763954877049344D^2+4647281343312980D-4001733231962720)\alpha_1}{3013527214512(D-3)(D-2)(D-1)} - \\
& \frac{21169201(5239853451D^3-42176800568D^2+111050449684D-95578515680)}{1506763607256(D-3)(D-2)(D-1)}, \alpha_2^2\alpha_1^3 - \\
& \frac{21169201(15864503101D^2-95188354942D+141021962832)\alpha_1}{1004509071504(D-3)^2} - \frac{97399493801(3D-8)(126539D-421026)}{502254535752(D-3)^2}, \\
& \alpha_1^2\alpha_2^3 - \frac{97399493801(3D-8)(126539D-421026)}{502254535752(D-3)^2} - \\
& \frac{21169201(15864503101D^2-95188354942D+141021962832)\alpha_1}{1004509071504(D-3)^2}, \\
& \alpha_1\alpha_2^4 - \frac{21169201(5239853451D^3-42176800568D^2+111050449684D-95578515680)}{1506763607256(D-3)(D-2)(D-1)} - \\
& \frac{4601(218977736303103D^3-1763954877049344D^2+4647281343312980D-4001733231962720)\alpha_1}{3013527214512(D-3)(D-2)(D-1)}, \alpha_2^2\alpha_1^4 - \\
& \frac{21169201(662990479498665D^3-4872230078680774D^2+11258936570700304D-7949126000914176)\alpha_1}{1741818729987936(D-3)^2(D-1)} - \\
& \frac{97399493801(15864503101D^3-116488195718D^2+269017828048D-189859148544)}{870909364993968(D-3)^2(D-1)}, \\
& \alpha_1^3\alpha_2^3 - \frac{97399493801(3D-8)(5336927395D^2-24840945214D+23503660472)\alpha_1}{193535414443104(D-3)^2(D-2)} - \\
& \frac{97399493801(15864503101D^3-116049358466D^2+266387477208D-185965500096)}{870909364993968(D-3)^2(D-2)}, \\
& \alpha_1^2\alpha_2^4 - \frac{97399493801(15864503101D^3-116488195718D^2+269017828048D-189859148544)}{870909364993968(D-3)^2(D-1)} - \\
& \frac{21169201(662990479498665D^3-4872230078680774D^2+11258936570700304D-7949126000914176)\alpha_1}{1741818729987936(D-3)^2(D-1)}, \\
& \alpha_{1,ct}^2 - \frac{\mu_{11}}{D-4}, \alpha_{2,ct}^2 - \frac{\mu_{22}}{D-4}, \alpha_1 \left(\alpha_{1,ct}^2 - \frac{\mu_{11}}{D-4} \right), \alpha_1 \left(\alpha_{2,ct}^2 - \frac{\mu_{22}}{D-4} \right), \alpha_2 \left(\alpha_{1,ct}^2 - \frac{\mu_{11}}{D-4} \right), \\
& \alpha_2 \left(\alpha_{2,ct}^2 - \frac{\mu_{22}}{D-4} \right), \alpha_1^2 \left(\alpha_{1,ct}^2 - \frac{\mu_{11}}{D-4} \right), \alpha_1^2 \left(\alpha_{2,ct}^2 - \frac{\mu_{22}}{D-4} \right), \alpha_1\alpha_2 \left(\alpha_{1,ct}^2 - \frac{\mu_{11}}{D-4} \right), \\
& \alpha_1\alpha_2 \left(\alpha_{2,ct}^2 - \frac{\mu_{22}}{D-4} \right), \alpha_{1,ct}^4 - \frac{\mu_{11}^2}{(D-4)(D-2)}, \alpha_{2,ct}^2 \left(\alpha_{1,ct}^2 - \frac{\mu_{11}}{D-4} \right), \dots
\end{aligned}$$

$$\begin{aligned}
& \left(\alpha_{1,ct}^2 - \frac{\mu_{11}}{D-4} \right) \left(\alpha_{2,ct}^2 - \frac{\mu_{22}}{D-4} \right), \alpha_2^2 \left(\alpha_{2,ct}^2 - \frac{\mu_{22}}{D-4} \right), \alpha_{2,ct}^4 - \frac{\mu_{22}^2}{(D-4)(D-2)}, \alpha_1^3 \left(\alpha_{2,ct}^2 - \frac{\mu_{22}}{D-4} \right), \\
& \alpha_1^2 \alpha_2 \left(\alpha_{1,ct}^2 - \frac{\mu_{11}}{D-4} \right), \alpha_1^2 \alpha_2 \left(\alpha_{2,ct}^2 - \frac{\mu_{22}}{D-4} \right), \alpha_1 \alpha_2^2 \left(\alpha_{1,ct}^2 - \frac{\mu_{11}}{D-4} \right), \\
& \alpha_1 \left(\alpha_{1,ct}^2 - \frac{\mu_{11}}{D-4} \right) \left(\alpha_{2,ct}^2 - \frac{\mu_{22}}{D-4} \right), \alpha_1 \alpha_2^2 \left(\alpha_{2,ct}^2 - \frac{\mu_{22}}{D-4} \right), \alpha_1 \left(\alpha_{2,ct}^4 - \frac{\mu_{22}^2}{(D-4)(D-2)} \right), \\
& \alpha_2 \left(\alpha_{1,ct}^4 - \frac{\mu_{11}^2}{(D-4)(D-2)} \right), \alpha_2^3 \left(\alpha_{1,ct}^2 - \frac{\mu_{11}}{D-4} \right), \alpha_2 \left(\alpha_{1,ct}^2 - \frac{\mu_{11}}{D-4} \right) \left(\alpha_{2,ct}^2 - \frac{\mu_{22}}{D-4} \right), \\
& \alpha_1^4 \left(\alpha_{2,ct}^2 - \frac{\mu_{22}}{D-4} \right), \alpha_1^3 \alpha_2 \left(\alpha_{2,ct}^2 - \frac{\mu_{22}}{D-4} \right), \alpha_1^2 \alpha_2^2 \left(\alpha_{1,ct}^2 - \frac{\mu_{11}}{D-4} \right), \\
& \alpha_1^2 \left(\alpha_{1,ct}^2 - \frac{\mu_{11}}{D-4} \right) \left(\alpha_{2,ct}^2 - \frac{\mu_{22}}{D-4} \right), \alpha_1^2 \alpha_2^2 \left(\alpha_{2,ct}^2 - \frac{\mu_{22}}{D-4} \right), \alpha_1^2 \left(\alpha_{2,ct}^4 - \frac{\mu_{22}^2}{(D-4)(D-2)} \right), \\
& \alpha_1 \alpha_2^3 \left(\alpha_{1,ct}^2 - \frac{\mu_{11}}{D-4} \right), \alpha_1 \alpha_2 \left(\alpha_{1,ct}^2 - \frac{\mu_{11}}{D-4} \right) \left(\alpha_{2,ct}^2 - \frac{\mu_{22}}{D-4} \right), \\
& \alpha_2^2 \left(\alpha_{1,ct}^4 - \frac{\mu_{11}^2}{(D-4)(D-2)} \right), \left(\alpha_{1,ct}^4 - \frac{\mu_{11}^2}{(D-4)(D-2)} \right) \left(\alpha_{2,ct}^2 - \frac{\mu_{22}}{D-4} \right), \alpha_2^4 \left(\alpha_{1,ct}^2 - \frac{\mu_{11}}{D-4} \right), \\
& \alpha_2^2 \left(\alpha_{1,ct}^2 - \frac{\mu_{11}}{D-4} \right) \left(\alpha_{2,ct}^2 - \frac{\mu_{22}}{D-4} \right), \left(\alpha_{1,ct}^2 - \frac{\mu_{11}}{D-4} \right) \left(\alpha_{2,ct}^4 - \frac{\mu_{22}^2}{(D-4)(D-2)} \right), \alpha_{1,ct}, \alpha_{2,ct}, \alpha_1 \alpha_{1,ct}, \\
& \alpha_1 \alpha_{2,ct}, \alpha_2 \alpha_{1,ct}, \alpha_{1,ct} \alpha_{2,ct}, \alpha_2 \alpha_{2,ct}, \alpha_1^2 \alpha_{1,ct}, \alpha_1^2 \alpha_{2,ct}, \alpha_1 \alpha_2 \alpha_{1,ct}, \alpha_1 \alpha_{1,ct} \alpha_{2,ct}, \alpha_1 \alpha_2 \alpha_{2,ct}, \\
& \alpha_{1,ct}^3, \alpha_{1,ct}^2 \alpha_{2,ct}, \alpha_2^2 \alpha_{1,ct}, \alpha_2 \alpha_{1,ct} \alpha_{2,ct}, \alpha_{1,ct} \alpha_{2,ct}^2, \alpha_2^2 \alpha_{2,ct}, \alpha_{2,ct}^3, \alpha_1^3 \alpha_{1,ct}, \alpha_1^3 \alpha_{2,ct}, \alpha_1^2 \alpha_2 \alpha_{1,ct}, \\
& \alpha_1^2 \alpha_{1,ct} \alpha_{2,ct}, \alpha_1^2 \alpha_2 \alpha_{2,ct}, \alpha_1 \alpha_{1,ct}^3, \alpha_1 \alpha_{1,ct}^2 \alpha_{2,ct}, \alpha_1 \alpha_2^2 \alpha_{1,ct}, \alpha_1 \alpha_2 \alpha_{1,ct} \alpha_{2,ct}, \alpha_1 \alpha_{1,ct} \alpha_{2,ct}^2, \\
& \alpha_1 \alpha_2^2 \alpha_{2,ct}, \alpha_1 \alpha_{2,ct}^3, \alpha_2 \alpha_{1,ct}^3, \alpha_{1,ct}^3 \alpha_{2,ct}, \alpha_2 \alpha_{1,ct}^2 \alpha_{2,ct}, \alpha_2^3 \alpha_{1,ct}, \alpha_2^2 \alpha_{1,ct} \alpha_{2,ct}, \alpha_2 \alpha_{1,ct} \alpha_{2,ct}^2, \\
& \alpha_{1,ct} \alpha_{2,ct}^3, \alpha_{2,ct}^3 \alpha_{2,ct}, \alpha_2 \alpha_{2,ct}^3, \alpha_1^4 \alpha_{2,ct}, \alpha_1^3 \alpha_2 \alpha_{1,ct}, \alpha_1^3 \alpha_{1,ct} \alpha_{2,ct}, \alpha_1^3 \alpha_2 \alpha_{2,ct}, \alpha_1^2 \alpha_{1,ct}^2 \alpha_{2,ct}, \\
& \alpha_1^2 \alpha_2^2 \alpha_{1,ct}, \alpha_1^2 \alpha_2 \alpha_{1,ct} \alpha_{2,ct}, \alpha_1^2 \alpha_{1,ct} \alpha_{2,ct}^2, \alpha_1^2 \alpha_2^3 \alpha_{2,ct}, \alpha_1^2 \alpha_2 \alpha_{1,ct}^3, \alpha_1 \alpha_2 \alpha_{1,ct}^3 \alpha_{2,ct}, \alpha_1 \alpha_{1,ct} \alpha_{2,ct}^3, \alpha_1 \alpha_2 \alpha_{2,ct}^3, \\
& \alpha_{1,ct}^4 \alpha_{2,ct}, \alpha_{2,ct}^4 \alpha_{1,ct}, \alpha_2 \alpha_{1,ct}^3 \alpha_{2,ct}, \alpha_{1,ct}^3 \alpha_2^2 \alpha_{2,ct}, \alpha_2^2 \alpha_{1,ct}^2 \alpha_{2,ct}, \alpha_{1,ct}^2 \alpha_{2,ct}^3, \alpha_2^4 \alpha_{1,ct}, \alpha_2^3 \alpha_{1,ct} \alpha_{2,ct}, \\
& \alpha_2^2 \alpha_{1,ct} \alpha_{2,ct}^2, \alpha_2 \alpha_{1,ct} \alpha_{2,ct}^3, \alpha_{1,ct} \alpha_2 \alpha_{2,ct}^4, \alpha_1^4 \alpha_2 \alpha_{2,ct}, \alpha_1^3 \alpha_2^2 \alpha_{1,ct}, \alpha_1^3 \alpha_2 \alpha_{1,ct} \alpha_{2,ct}, \alpha_1^3 \alpha_{1,ct} \alpha_{2,ct}^2, \\
& \alpha_1^3 \alpha_2^2 \alpha_{2,ct}, \alpha_1^3 \alpha_2^3 \alpha_{2,ct}, \alpha_1^2 \alpha_2 \alpha_{1,ct}^2 \alpha_{2,ct}, \alpha_1^2 \alpha_2^3 \alpha_{1,ct}, \alpha_1^2 \alpha_2^2 \alpha_{1,ct} \alpha_{2,ct}, \alpha_1^2 \alpha_2 \alpha_{1,ct} \alpha_{2,ct}^2, \alpha_1^2 \alpha_{1,ct} \alpha_{2,ct}^3, \\
& \alpha_1^2 \alpha_2^3 \alpha_{2,ct}, \alpha_1^2 \alpha_2 \alpha_{2,ct}^3, \alpha_1 \alpha_2^2 \alpha_{1,ct}^3, \alpha_1 \alpha_2 \alpha_{1,ct}^3 \alpha_{2,ct}, \alpha_1 \alpha_{1,ct}^3 \alpha_{2,ct}^2, \alpha_1 \alpha_2^2 \alpha_{1,ct}^2 \alpha_{2,ct}, \alpha_1 \alpha_{1,ct}^2 \alpha_{2,ct}^3, \\
& \alpha_1 \alpha_2^4 \alpha_{1,ct}, \alpha_1 \alpha_2^3 \alpha_{1,ct} \alpha_{2,ct}, \alpha_1 \alpha_2^2 \alpha_{1,ct} \alpha_{2,ct}^2, \alpha_1 \alpha_2 \alpha_{1,ct} \alpha_{2,ct}^3, \alpha_1 \alpha_{1,ct} \alpha_{2,ct}^4, \alpha_2 \alpha_{1,ct}^4 \alpha_{2,ct}, \alpha_2^3 \alpha_{1,ct}^3, \\
& \alpha_2^2 \alpha_{1,ct}^3 \alpha_{2,ct}, \alpha_2 \alpha_{1,ct}^3 \alpha_{2,ct}^2, \alpha_{1,ct}^3 \alpha_{2,ct}^3, \alpha_2^3 \alpha_{1,ct}^2 \alpha_{2,ct}, \alpha_2 \alpha_{1,ct}^2 \alpha_{2,ct}^3 \} \}
\end{aligned}$$

Acknowledgments

I would like to thank Dr. Takemichi Okui, Dr. Olmo Zavala-Romero, and Dr. Rachel Yohay for their support and service on the senior thesis committee. Their review and support of this work throughout the writing process has been invaluable. Additionally, the education each has provided to me made this thesis possible. I would like to thank Dr. Takemichi Okui for his instruction on general and special relativity and for deepening my knowledge of high energy physics, which form the basis of this research. I would like to thank Dr. Olmo Zavala-Romero for his instruction in scientific computing, which was very helpful in the computations used in this project and his introduction to github. Further, I would like to thank Dr. Rachel Yohay for her introduction to the field of High Energy research and her instruction introducing me to the field.

Additionally, we would like to thank Gustavo Figueiredo and Irene Roman for there support throughout various stages of this work, including meeting with me several times to help fix issues with my code and to help me understand new concepts.

Finally, I thank Dr. Fernando Febres Cordero for his mentorship throughout this project. His instruction has been vital for completing this project and will serve me into my future research.

References

- [1] S. Abreu, J. Dormans, F. Febres Cordero, H. Ita, M. Kraus, B. Page, E. Pascual, M. S. Ruf, and V. Sotnikov. Caravel: A C++ framework for the computation of multi-loop amplitudes with numerical unitarity. *Comput. Phys. Commun.*, 267:108069, 2021.
- [2] S. Abreu, F. Febres Cordero, H. Ita, M. Jaquier, B. Page, M. S. Ruf, and V. Sotnikov. Two-Loop Four-Graviton Scattering Amplitudes. *Phys. Rev. Lett.*, 124(21):211601, 2020.
- [3] Samuel Abreu, Ruth Britto, and Claude Duhr. The SAGEX review on scattering amplitudes chapter 3: Mathematical structures in feynman integrals. *Journal of Physics A: Mathematical and Theoretical*, 55(44):443004, nov 2022.
- [4] Samuel Abreu, Fernando Febres Cordero, Harald Ita, Ben Page, and Mao Zeng. Planar Two-Loop Five-Gluon Amplitudes from Numerical Unitarity. *Phys. Rev. D*, 97(11):116014, 2018.
- [5] Javier M. Antelis and Claudia Moreno. Obtaining gravitational waves from inspiral binary systems using LIGO data. *Eur. Phys. J. Plus*, 132(1):10, 2017. [Erratum: Eur.Phys.J.Plus 132, 103 (2017)].
- [6] Thomas Bitoun, Christian Bogner, René Pascal Klausen, and Erik Panzer. Feynman integral relations from parametric annihilators. *Letters in Mathematical Physics*, 109(3):497–564, aug 2018.
- [7] Alessandra Buonanno, Mohammed Khalil, Donal O’Connell, Radu Roiban, Mikhail P. Solon, and Mao Zeng. Snowmass White Paper: Gravitational Waves and Scattering Amplitudes. In *Snowmass 2021*, 4 2022.
- [8] F. Febres Cordero. Qcd for precision studies at the lhc, 2023.
- [9] John F. Donoghue, Mikhail M. Ivanov, and Andrey Shkerin. Epfl lectures on general relativity as a quantum field theory, 2017.
- [10] R. Keith Ellis, Zoltan Kunszt, Kirill Melnikov, and Giulia Zanderighi. One-loop calculations in quantum field theory: from Feynman diagrams to unitarity cuts. *Phys. Rept.*, 518:141–250, 2012.
- [11] Fernando Febres Cordero, Manfred Kraus, Guanda Lin, Michael S. Ruf, and Mao Zeng. Conservative Binary Dynamics with a Spinning Black Hole at $\mathcal{O}(\text{G}^3)$ from Scattering Amplitudes. *Phys. Rev. Lett.*, 130(2):021601, 2023.
- [12] Janusz Gluza, Krzysztof Kajda, and David A. Kosower. Towards a basis for planar two-loop integrals. *Physical Review D*, 83(4), feb 2011.
- [13] Ben Gripaios. Lectures: From quantum mechanics to the standard model, 2020.
- [14] Laporta. *International Journal of Modern Physics A*, 15:5087, 2000.
- [15] Irene Marie Roman. Multi-loop scattering amplitudes in qcd and gravity. *FSU PhD prospectus*, apr 2022.
- [16] A. V. Smirnov and A. V. Petukhov. The number of master integrals is finite, 2010.
- [17] A.V. Smirnov and F.S. Chukharev. Fire6: Feynman integral reduction with modular arithmetic. *Computer Physics Communications*, 247:106877, February 2020.
- [18] Stefan Weinzierl. Feynman integrals, 2022.
- [19] Nadia L. Zakamska. Theory of special relativity, 2018.